Based on these findings, the female rats were hypothesized to be a good animal model with which to evaluate the pharmacokinetic significance of the luminal organic cation transport system, avoiding the influence of hormonal regulation of the basolateral rOCT2. In the present study, we examined the renal handling of cimetidine, a substrate for the renal organic cation transport system, in rats after Nx. Furthermore, the expression levels of renal organic ion transporers were examined to clarify the responsible factor in the tubular secretion of cationic drugs in the kidney.

2. Materials and methods

2.1. Experimental animals

For ablation of the renal mass, male and female Wistar albino rats (180–200 g) were anesthetized with sodium pentobarbital (50 mg/kg) and the kidneys were exposed under aseptic conditions via a ventral abdominal incision. The right kidney was removed, the posterior and anterior apical segmental branches of the left renal artery were individually ligated, and the abdominal incision was closed with 4-0 silk sutures. In the sham-operated animals, the peritoneal cavity was exposed, and both kidneys were gently manipulated. To examine the effect of the administration of testosterone on drug pharmacokinetics and the renal expression of transporters, the sham-operated and Nx rats were administered a subcutaneous injection of testosterone (0.5 mg testosterone enanthate (T) dissolved in 200 μL corn oil/rat, T(+)) or vehicle (200 μL corn oil/rat, T(−)) at 1, 4, 7, 10 and 13 days after surgery. Except during the subcutaneous administration of testosterone every 3 days, animals were allowed access to water and standard rat chow for 2 weeks.

Rats were maintained in metabolic cages for 24 h before the in vivo experiment, to determine urine output and urinary levels of creatinine. The blood urea nitrogen (BUN) concentration was determined by the urease/indophenol method. The levels of creatinine in plasma and urine were determined with the Jaffé reaction. For measurements, we used assay kits from Wako Pure Chemical Industries (Osaka, Japan). The plasma testosterone and 17β-esrtadiol level was measured with an enzyme immunoassay kit (Cayman Chemical Co., MI, USA). The experiments with animals were performed in accordance with the *Guidelines for Animal Experiments of Kyoto University*.

2.2. Infusion experiment

Rats were anesthetized with an intraperitoneal administration of 50 mg/kg sodium pentobarbital. Catheters were inserted into the right femoral artery and the left femoral vein with polyethylene tubing (Intramedic PE-50, Becton Dickinson and Co., Parsippany, NJ, USA) filled with a heparin solution (100 U/mL) for blood sampling and drug administration, respectively. Urine was collected from the urinary bladder catheterized with PE-50 tubing. Thereafter, cimetidine was administered as a bolus via the femoral vein and incorporated into the infusion solution as described [12]. The loading and maintenance doses of cimetidine including 4% mannitol were 317 μmol/kg and 21.8 μmol/mL, respectively. The infusion rate was 2.2 mL/h using an automatic infusion pump (Natsume Saisakusho, Tokyo, Japan). Mannitol was used to maintain a sufficient and constant urine flow rate. After a 30-min equilibration period, urine samples were collected three times at 10 min intervals, and blood samples were obtained at the midpoint of urine collection. The plasma was immediately separated from erythrocytes by centrifugation. At the end of the experiment, an adequate volume of blood was collected from the abdominal aorta to examine the plasma protein binding rate, and the kidneys were removed to determine the tissue concentrations of cimetidine and the expression of renal drug transporters. The concentrations of cimetidine in plasma, urine, and the renal homogenate were determined by high performance liquid chromatography [13]. The plasma unbound fraction (fu) of cimetidine was determined by ultrafiltration using a micropartition system (MRS-1, Amicon Inc., Beverly, MA, USA), as described [12]. The free fraction of cimetidine was expressed as the ratio of the concentration in the ultrafiltrate to that in plasma.

2.3. Analytical methods

Pharmacokinetic parameters were calculated using standard procedures for each experimental period. The total plasma clearance (Ctot) was calculated by dividing the infusion rate by the steady-state plasma concentration (Cpss) at the midpoint of urine collection. Renal clearance (Cren) was obtained by dividing the urinary excretion rate by Cpss. The renal clearance of unbound cimetidine (Cr.f) was determined by dividing Cren by the fu of cimetidine. The glomerular filtration rate (GFR) was assumed to be equal to the Cren of creatinine. The renal secretory clearance of unbound cimetidine was calculated by substracting GFR from Cr.f.

2.4. Polyclonal antibody against rMATE1 and Western blot analysis

Polyclonal antibody was raised against the synthetic peptide that corresponded to the C-terminus of MATE1, which is fully conserved in human and rat [8]. The crude plasma membrane fractions were prepared from rat kidneys, as described previously [14]. The crude plasma membrane fractions were separated by 10% sodium dodecyl sulfate-polyacrylamide gel electrophoresis (SDS-PAGE) and transferred onto polyvinylidene difluoride membranes (Immobilon-P, Millipore, Bedford, MA, USA) by semi-dry electroblotting. The blots were blocked with 5% non-fat dry milk and 5% bovine serum albumin in phosphate-buffered saline (PBS, 137 mM NaCl, 3 mM KCl, 8 mM Na_2HPO_4, 1 mM KH_2PO_4, and 12 mM K_2HPO_4, pH 7.5) containing 0.5% Tween 20 (PBS-T) for OAT1, OAT3, OCT1, OCT2 and Na^+/K^+-ATPase or 5% non-fat dry milk in Tris-buffered saline (TBS, 20 mM Tris and 137 mM NaCl) containing 0.5% Tween 20 (TBS-T) for MATE1. The blots were then incubated overnight at 4 °C with primary antibody specific for rOAT1[11], rOAT3 [11], rOCT1 [15], rOCT2 [9], rMATE, NHE3 (CHEMICON International Inc., Temecula, CA, USA), Na^+/K^+-ATPase (Upstate Biotechnology Inc., Lake Placid, NY, USA), or with an antibody preabsorbed with the synthetic antigen peptide (20 μg/mL) for rMATE1. The blots were washed three times with PBS-T or TBS-T, and the bound antibody was detected on X-ray film by enhanced chemiluminescence (ECL) with

horseradish peroxidase-conjugated secondary antibodies and cyclic diacylhydrazides (GE Healthcare Bio-Sciences Corp., Piscataway, NJ, USA). Na^+/K^+-ATPase was examined as a positive control. The relative amounts of the bands in each lane were determined densitometrically using NIH Image 1.61 (National Institutes of Health, Bethesda, MD), and the densitometric ratios relative to each control (Sham or Sham T(−)) were used as the reference and accorded an arbitrary value of 1.0, respectively.

2.5. *Immunohistochemical analysis*

The animals were anesthetized and the kidneys were perfused via the abdominal aorta, first with saline containing 50 U/mL of heparin and then with 4% paraformaldehyde in PBS. Fixed tissues were embedded in OCT compound (Sakura Finetechnical, Tokyo, Japan) and frozen rapidly in liquid nitrogen. Sections (5 μm thick) were cut and covered with a blocking agent Blocking One® (Nacalai Tesque, Kyoto, Japan) containing 1 mg/mL RNase A (Nacalai Tesque) at 37 °C for 30 min. The covered sections were incubated at 37 °C for 60 min with antiserum specific for MATE1 (1:100 dilution) or anti-NHE3 antibody (1:200). Following two washings each with 3 × PBS and regular PBS, sections were incubated with Cy3-labeled donkey anti-rabbit IgG (CALTAG Laboratory, San Francisco, CA, USA), Alexa 488-Phalloidin (Molecular Probe, Eugene, OR, USA), and 4′,6-diamidino-2-phenylindole (DAPI; Wako, Osaka, Japan) at 37 °C for 60 min. These sections were examined and captured with a BZ-8000 (KEYENCE, Osaka, Japan) at 150× magnification.

2.6. *Statistical analysis*

All data are expressed as means ± S.E. Data from the Western blot analysis are expressed in arbitrary units of densitometry/25 μg protein. Comparisons were made using the unpaired *t*-test. $P < 0.05$ was considered significant.

3. Results

3.1. *Renal functional data after administration of testosterone in female rats with chronic renal failure*

As shown in Table 1, body weight tended to decline and 24 h urine volume was markedly increased in female Nx rats. The levels of BUN and creatinine in plasma (Pcr) were significantly increased, and the creatinine clearance (Ccr) was markedly decreased in female Nx rats in comparison with sham-operated controls. These parameters were consistent with our previous report using male Nx rats [11]. Unlike in the male rats, plasma level of testosterone was comparable between female sham-operated rats and Nx rats. Although an elevation in the plasma level of testosterone on the administration of testosterone was confirmed to occur both in sham-operated and in Nx rats, the plasma concentration of 17β-estradiol was not significantly changed. In addition, none of the renal functional data changed significantly after the administration of testosterone in female rats.

3.2. *Pharmacokinetics of cimetidine after administration of testosterone in female rats with chronic renal failure*

Table 2 shows the pharmacokinetic parameters of cimetidine in female rats with or without treatment with testosterone. The steady-state plasma concentration (Cpss) of cimetidine was markedly elevated in the Nx rats in comparison with sham-operated controls. The total plasma clearance (Ctot) of cimetidine was significantly decreased in female Nx rats compared with the controls. The renal clearance (Cren) of cimetidine in female sham-operated rats was about 60% of that in male sham-operated rats according to our previous report [11]. In female rats, the Cren of cimetidine was markedly decreased by Nx to 43% of that in the sham-operated controls. The ratio between the renal concentration and Cpss of cimetidine (Kp) was shown to be significantly decreased in Nx females compared to the sham-operated controls. Similar to the renal functional data in Table 1, there was no significant influence on the pharmacokinetic parameters of cimetidine in female rats with or without the administration of testosterone.

As shown in Fig. 1, the tubular secretory clearance (Csec) of cimetidine in female sham-operated rats was about 50% of that in the sham-operated males. In male and female Nx rats, it was markedly decreased. After the administration of testosterone, the Csec of cimetidine in male Nx rats recovered significantly to be 80% of that in male controls, but that in female Nx rats did not change at all.

3.3. *Gender difference in protein expression of rOCT2, rMATE1 and NHE3*

At first, a primary band with a size of 66 kDa was detected using the antibody raised against rMATE1 (Fig. 2(A)). The

Table 1 – Renal functional data and plasma testosterone and 17β-estradiol levels after the administration of testosterone in female rats

	Body weight (g)	Urine volume (mL/24 h)	Pcr (mg/dL)	Ccr (mL/min kg)	BUN (mg/dL)	Testosterone (ng/mL)	17β-Estradiol (pg/mL)
Sham T(−)	212 ± 10	18.2 ± 2.2	0.52 ± 0.08	6.0 ± 1.0	16.7 ± 0.7	0.1 ± 0.0	51.3 ± 10.1
Sham T(+)	228 ± 9	17.8 ± 2.0	0.55 ± 0.07	5.2 ± 0.8	18.1 ± 0.9	5.5 ± 0.7**	30.1 ± 14.4
Nx T(−)	199 ± 7	30.3 ± 5.4**	1.20 ± 0.12**	2.3 ± 0.3**	59.4 ± 5.6**	0.2 ± 0.0	58.6 ± 14.4
Nx T(+)	207 ± 6	31.7 ± 3.3**	1.12 ± 0.11**	2.4 ± 0.3**	58.7 ± 5.3**	5.0 ± 0.6**	38.7 ± 8.3

Values are means ± S.E. for 6–10 rats; Pcr, plasma creatinine; Ccr, creatinine clearance; BUN, blood urea nitrogen; Sham T(−), sham-operated rats administered vehicle; Sham T(+), sham-operated rats administered testosterone, Nx T(−), 5/6 nephrectomized rats administered vehicle; Nx T(+), 5/6 nephrectomized rats administered testosterone. **$P < 0.01$, significantly different from Sham T(−) rats.

Table 2 – Pharmacokinetic parameters of cimetidine in infusion experiments after the administration of testosterone in female rats

	Cpss (μmol/L)	fu	Ctot (mL/min kg)	Cren (mL/min g kid)	Kp
Sham T(−)	254 ± 12	0.74 ± 0.04	15.5 ± 0.9	1.4 ± 0.1	1.6 ± 0.0
Sham T(+)	260 ± 20	0.76 ± 0.01	13.8 ± 0.6	1.4 ± 0.2	1.6 ± 0.1
Nx T(−)	409 ± 17**	0.70 ± 0.05	9.5 ± 0.3**	0.6 ± 0.1**	0.9 ± 0.1**
Nx T(+)	405 ± 30**	0.78 ± 0.04	9.4 ± 0.7**	0.6 ± 0.2**	1.0 ± 0.1**

Each value represents the mean ± S.E. of six rats; Cpss, steady-state plasma concentration; Ctot, total clearance; Cren, renal clearance; fu, plasma unbound fraction; Kp, tissue to plasma concentration ratio. Sham T(−), sham-operated rats administered vehicle; Sham T(+), sham-operated rats administered testosterone, Nx T(−), 5/6 nephrectomized rats administered vehicle; Nx T(+), 5/6 nephrectomized rats administered testosterone. **$P < 0.01$, significantly different from Sham T(−) rats.

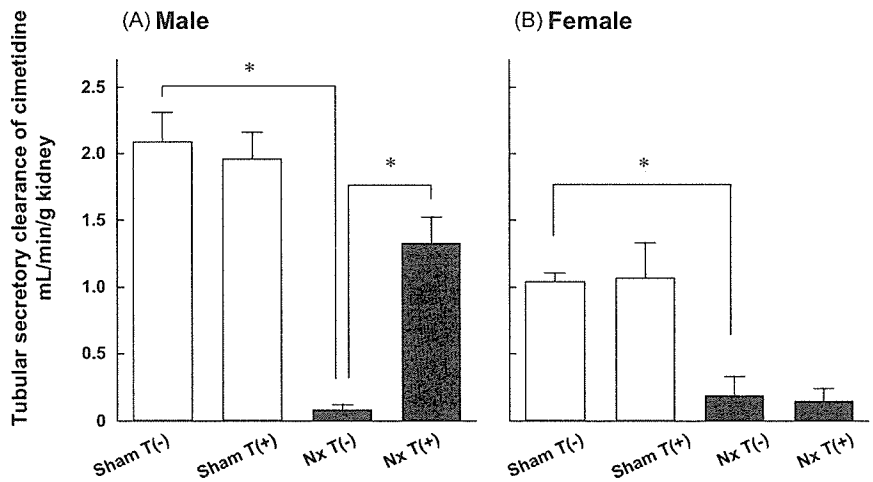

Fig. 1 – (A and B) Renal secretory clearance of unbound cimetidine. Cimetidine (21.8 μmol/mL) was infused at a rate of 2.2 mL/h using an automatic infusion pump. The renal secretory clearance was calculated by substracting GFR from Cr.f. Each column represents the mean ± S.E. for six rats. *Statistically significant difference. Sham T(−), sham-operated rats administered vehicle; Sham T(+), sham-operated rats administered testosterone enanthate; Nx T(−), 5/6 nephrectomized rats administered vehicle; Nx T(+), 5/6 nephrectomized rats administered testosterone enanthate.

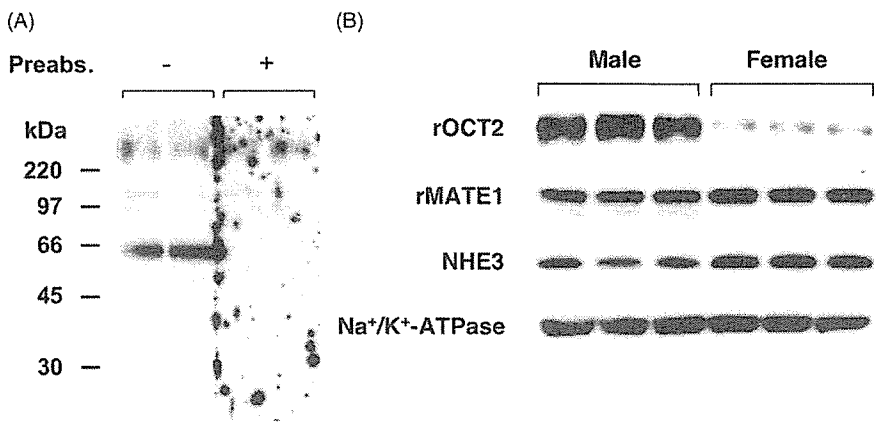

Fig. 2 – Protein expression of rOCT2, rMATE1, NHE3 and Na^+/K^+-ATPase in male and female rats. Crude plasma membrane fractions (25 μg) from total kidneys were separated by sodium dodecyl sulfate-polyacrylamide gel electrophoresis (10%) and blotted onto Immobilon® membranes. (A) The antisera (1:1000 dilution) for rMATE1 was preabsorbed (Preab.) with (+) or without (−) antigen peptide (20 μg/mL) of rMATE1. (B) Antisera specific for rOCT2, rMATE1, NHE3 and Na^+/K^+-ATPase (1:1000–10,000 dilution) were used as primary antibodies.

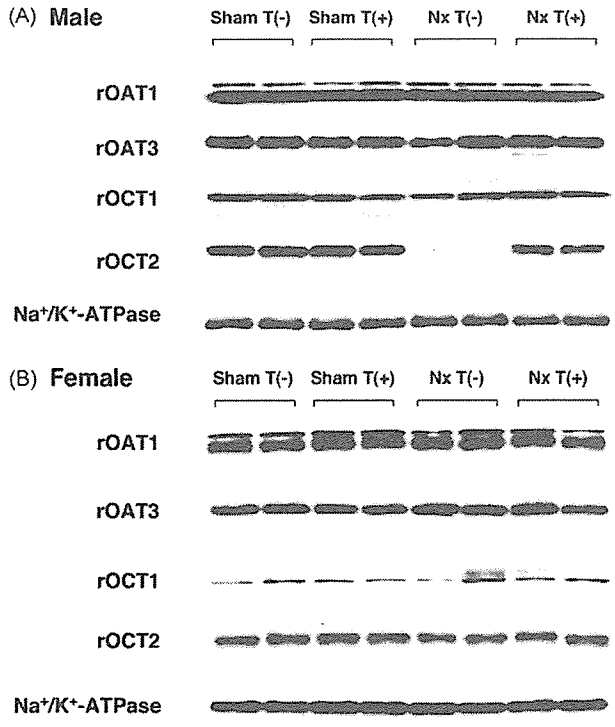

Fig. 3 – Protein expression of organic ion transporters in sham-operated and Nx rats after treatment with testosterone. Crude plasma membrane fractions (25 μg) from total kidneys were separated by sodium dodecyl sulfate-polyacrylamide gel electrophoresis (10%) and blotted onto Immobilon® membranes. The expression levels of various transporters in male (A) and female (B) rats. Antisera specific for rOAT1, rOAT3, rOCT1, rOCT2, and Na^+/K^+-ATPase (1:1000–10,000 dilution) were used as primary antibodies. Sham T(−), sham-operated rats administered vehicle; Sham T(+), sham-operated rats administered testosterone enanthate; Nx T(−), 5/6 nephrectomized rats administered vehicle; Nx T(+), 5/6 nephrectomized rats administered testosterone enanthate.

preabsorption of antibody with antigen peptide abolished this band, showing the presence of rMATE1 protein in the rat kidney. The level of rOCT2 in female rats was about 25% of that in male rats (Fig. 2(B)). On the other hand, the expression level of rMATE1 was comparable between sexes. The level of NHE3 was slightly, but not significantly, higher in female rats compared to male rats.

3.4. *Protein expression of basolateral organic ion transporters in Nx rats*

Consistent with our previous findings [11], the protein expression of rOCT2 was markedly depressed in male Nx rats, and recovered to around the control level with the administration of testosterone (T(+)) (Fig. 3(A)). In addition, there was no influence of Nx on the administration of testosterone on the expression levels of rOAT1, rOAT3, rOCT1 and Na^+/K^+-ATPase. In female rats, the levels of the basolateral organic ion transporters, rOAT1, rOAT3, rOCT1 and rOCT2, and Na^+/K^+-ATPase were not affected by Nx with or without the administration of testosterone (Fig. 3(B)).

Although the level of rOCT2 protein correlated well with the Csec of cimetidine in the male rats, no significant correlation was observed in the female rats (Fig. 4).

3.5. *Expressional change and pharmacokinetic significance of luminal rMATE1 and NHE3 in Nx rats*

Next, we examined the expressional change of the luminal H^+/organic cation antiporter rMATE1 and Na^+/H^+ exchanger 3 (NHE3), which generates an inward H^+-gradient at the brush-border membranes. Western blot analysis revealed that the levels of rMATE1 and NHE3 were markedly decreased by Nx in both male and female rats (Fig. 5).

The coefficient of correlation between the Csec of cimetidine and the level of rMATE1 was 0.72 ($P = 0.0037$) in male rats, whereas the data was relatively scattered (Fig. 6(A)). In contrast, the Csec of cimetidine showed better correlation

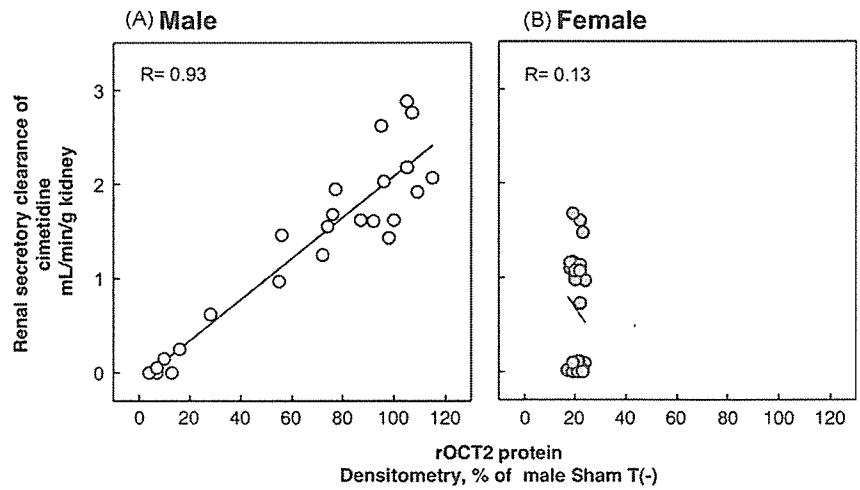

Fig. 4 – Correlation between rOCT2 expression and the renal clearance of cimetidine in rats. Correlation between the rOCT2 protein expression and renal secretory clearance of unbound cimetidine in male (A, open circles) and female rats (B, closed circles). The rOCT2 protein level was determined as outlined in Section 2. Sham T(−), sham-operated rats administered vehicle.

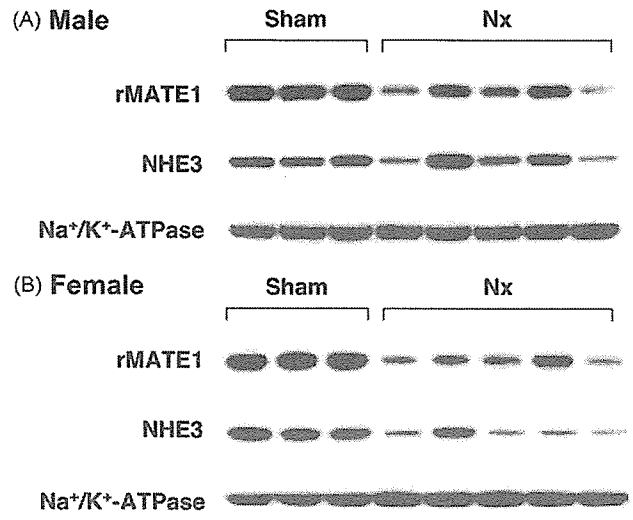

Fig. 5 – (A and B) Protein expression of rMATE1 and NHE3 in sham-operated and Nx rats. Crude plasma membrane fractions (25 μg) from total kidneys were separated by sodium dodecyl sulfate-polyacrylamide gel electrophoresis (10%) and blotted onto Immobilon® membranes. Antisera specific for rMATE1, NHE3, and Na^+/K^+-ATPase (1:1000 dilution) were used as primary antibodies. Sham, sham-operated rats; Nx, 5/6 nephrectomized rats.

with the level of rMATE1 protein in female rats ($r = 0.74$, $P = 0.0036$) (Fig. 6(B)).

3.6. *Immunohistochemical analysis of rMATE1 and NHE3*

An immunohistochemical analysis was performed to examine the localization of rMATE1 and NHE3 in female rats. Positive staining for rMATE1 and NHE3 was detected in the brush-border membranes of proximal tubules (Fig. 7(A) and (B)). Both rMATE1 and NHE3 was abundant in the renal cortex. In addition, it seemed that the localization of rMATE1 and NHE3 was not affected by Nx (Fig. 7(C)–(F)).

4. Discussion

Functional changes in renal organic ion transporters are of clinical relevance, particularly to the use of drugs with that are highly toxic and have a narrow therapeutic index. Serious kidney disease, such as chronic renal failure, will influence the renal disposition of organic ions and the expression of drug transporters. Our previous study demonstrated that the mRNA expression levels of OAT-K1 and OAT-K2 were markedly diminished after Nx, and the renal clearance of methotrexate was markedly decreased in Nx rats compared with sham-operated rats [16]. Furthermore, the renal secretion of cimetidine and the level of basolateral rOCT2 was also decreased under chronic renal failure in male rats, and the reduced plasma level of testosterone was considered to cause these phenomena [11]. Although two steps of transmembrane transport were thought to be involved in the vectorial secretion of cationic drugs, there has been no report about the luminal MATE1 in renal disease state. Sex-hormonal levels differ markedly between the genders, and recently transporters such as rOCT2, rOAT2 and oatp1 have been reported to exhibit gender differences in their expression in the rat kidney [9,17,18]. Based on these findings, we hypothesized that female rats would show significantly different changes in the urinary excretion of cimetidine and the expression of organic ion transporters during chronic renal failure, avoiding the influence of testosterone. In the present study, to obtain more information about the pharmacokinetic significance of cationic drug excretion systems focusing on luminal transporter, rMATE1, we have examined the renal excretion of the cationic substrate cimetidine and the expression of organic ion transporters in male and female Nx rats.

Consistent with previous findings, the decreased expression level of the renal rOCT2 and the Csec of cimetidine were recovered by the administration of testosterone in the male Nx

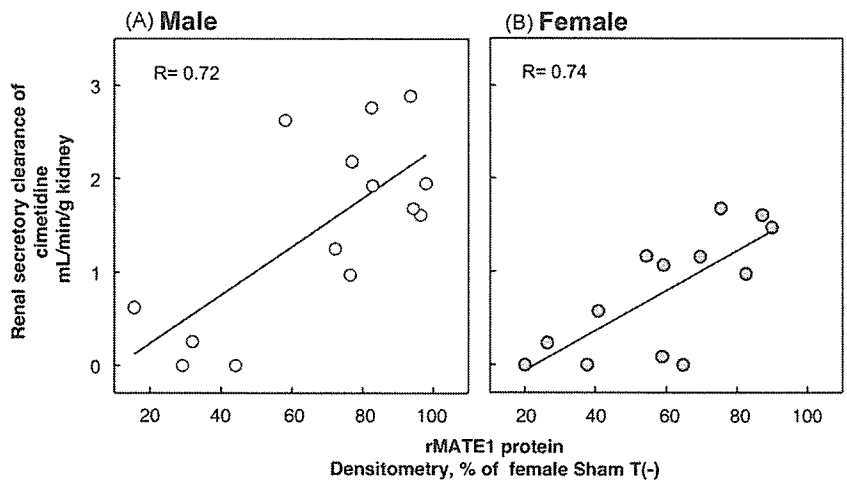

Fig. 6 – Correlation between rMATE1 expression and the renal clearance of cimetidine in rats. Correlation between the rMATE1 protein expression and renal secretory clearance of unbound cimetidine in male (A, open circles) and female rats (B, closed circles). The rMATE1 protein level was determined as outlined in Section 2. Sham T(−), sham-operated rats administered vehicle.

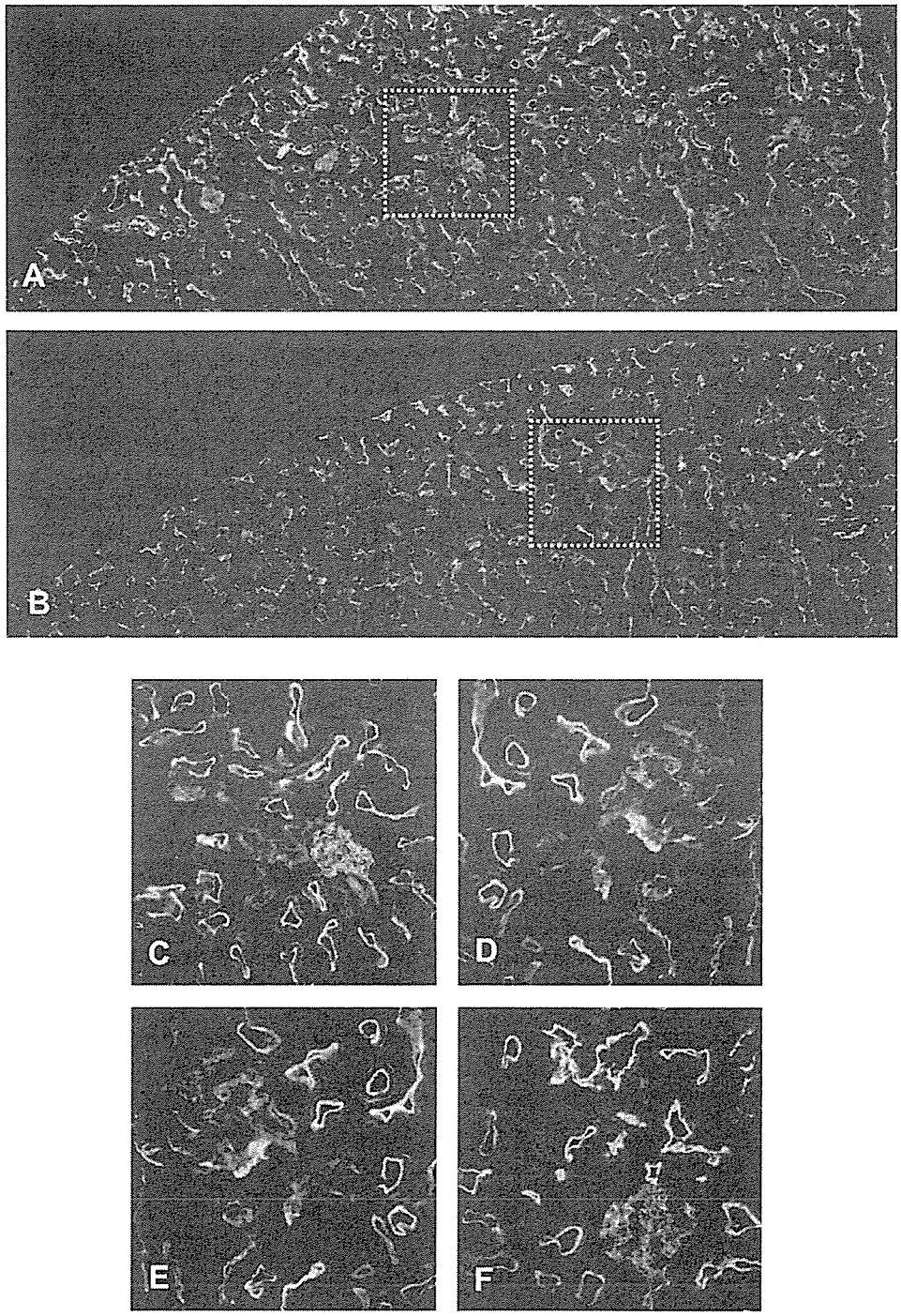

Fig. 7 – Immunohistochemistry of rMATE1 and NHE3 in female sham-operated and Nx rats. The rMATE1 or NHE3 (red), F-actin (green), and DAPI (blue) signals were merged in the same section. The yellow signals consisting of rMATE1 or NHE3 and F-actin were concentrated in the brush-border membranes of proximal tubules. The localization of rMATE1 (A) and NHE3 (B) in sham-operated rats were relatively condensed around the cortex. The luminal localization of rMATE1 (C and D) and NHE3 (E and F) in sham-operated (C and E) and in Nx (D and F) rats were confirmed. Magnification: 150×.

rats (Figs. 1(A) and 3(A)). In the female rats, the renal Csec of cimetidine was about 50% of that in the male rats (Fig. 1(B)). The expression levels of basolateral transporters were not affected by Nx and testosterone. In addition, no correlation was observed between the renal level of rOCT2 and the Csec of cimetidine (Fig. 4(B)). In infusion experiments, tissue to plasma concentration ratio (Kp) was significantly decreased in Nx rats. In Nx rats, the level of the tubular sodium transporters were markedly decreased and the plasma levels of sodium and potassium were significantly changed [19]. This suggested that the difference in the membrane potential at the basolateral side of renal epithelial cells were also changed and

the uptake of cationic drugs in epithelial cells was reduced, though the expressional change of rOCT2 was not observed. Considering these results, only the level of basolateral rOCT2 in the kidney could not explain the entire vectorial secretion of the cationic drugs.

Recently, the luminal H^+/organic cation antiporters, human (h) MATE1, hMATE2-K, rMATE1 and mouse MATE1 have been cloned and characterized [6–8,20]. rMATE1 was mainly expressed in the kidney and placenta, and suggested to be a major contributor to the tubular H^+/organic cation antiport activity in rats [7]. In contrast, hMATE2-K was isolated as a second member of the MATE family in the human kidney, despite no counterpart gene having been identified in rats [8]. Most recently, a platinum agent oxaliplatin was found to be a superior substrate for hMATE2-K rather than hMATE1, and therefore, the extensive tubular secretion of oxaliplatin via hMATE2-K were suggested to be a mechanism behind the lowered renal toxicity of the drug [21].

In the female as well as male rats, the level of rMATE1 was markedly depressed by the Nx (Fig. 5). In contrast to the level of basolateral rOCT2, the level of rMATE1 correlated well with the Csec of cimetidine in the female rats. Considering that there was no significant alteration to the expression of the basolateral transporters (rOAT1, rOAT3, rOCT1 and rOCT2) in the female rats following Nx, the luminal rMATE1 should play a crucial role in the tubular secretion of cimetidine in the female rats.

In the rat renal tubular brush-border membranes, the luminal secretion of cimetidine as well as tetraethyl ammonium was mediated by an electroneutral H^+/organic cation antiport system driven by an inward H^+-gradient, and that H^+-gradient was mainly created by NHE [22–24]. At the brush-border membranes of proximal tubules, the type 3 NHE are considered dominant among the NHE family [25,26]. In the present study, we also examined the expression level and membrane localization of NHE3 as well as rMATE1 in the female rats. The immunohistochemical analysis using antibodies specific for rMATE1 or NHE3 strongly suggested that both transporters cooperatively function on the luminal side of the proximal tubules, especially in the superficial cortex (Fig. 7(A) and (B)), i.e., rMATE1-mediated tubular secretion of cationic compounds could be driven by the NHE3-created inward H^+-gradient.

The expression of NHE3 was depressed after Nx in both the male and female rats (Fig. 5). Kwon et al. [19] showed that the level of the tubular sodium transporters including NHE3 were significantly decreased in Nx rats. Furthermore, they demonstrated that the localization of NHE3 was also found at the brush-border membranes in the Nx rats, which was comparable with our present results. Therefore, the decreased renal tubular secretion of cimetidine was not only due to the decreased in the expression of rMATE1, but also the functional loss of this transporter via a lowered H^+-gradient at the brush-border membrane, caused by the decrease in NHE3.

In conclusion, we have advanced our findings on the renal handling of cationic drugs, demonstrating that the level of luminal rMATE1 was markedly decreased during chronic renal failure, and rMATE1 as well as the basolateral rOCT2 played a crucial role in the vectorial transport of organic cations as detoxicating factors. In addition, the expression of NHE3 was also depressed in Nx rats, and the localization of NHE3 was similar to that of rMATE1, suggesting the expression level of NHE3 might affect rMATE1 activity by creating an inward H^+-gradient.

Acknowledgments

This work was supported in part by a grant-in-aid for Research on Advanced Medical Technology from the Ministry of Health, Labor and Welfare of Japan, by the Japan Health Science Foundation "Research on Health Sciences Focusing on Drug Innovation", by a grant-in-aid for Scientific Research from the Ministry of Education, Science, Culture and Sports of Japan, and by the 21st Century COE program "Knowledge Information Infrastructure for Genome Science".

REFERENCES

[1] Grundemann D, Gorboulev V, Gambaryan S, Veyhl M, Koepsell H. Drug excretion mediated by a new prototype of polyspecific transporter. Nature 1994;372:549–52.
[2] Okuda M, Saito H, Urakami Y, Takano M, Inui K. cDNA cloning and functional expression of a novel rat kidney organic cation transporter OCT2. Biochem Biophys Res Commun 1996;224:500–7.
[3] Sekine T, Watanabe N, Hosoyamada M, Kanai Y, Endou H. Expression cloning and characterization of a novel multispecific organic anion transporter. J Biol Chem 1997;272:18526–9.
[4] Kusuhara H, Sekine T, Utsunomiya-Tate N, Tsuda M, Kojima R, Cha SH, et al. Molecular cloning and characterization of a new multispecific organic anion transporter from rat brain. J Biol Chem 1999;274:13675–80.
[5] Inui K, Masuda S, Saito H. Cellular and molecular aspects of drug transport in the kidney. Kidney Int 2000;58:944–58.
[6] Otsuka M, Matsumoto T, Morimoto R, Arioka S, Omote H, Moriyama Y. A human transporter protein that mediates the final excretion step for toxic organic cations. Proc Natl Acad Sci USA 2005;102:17923–8.
[7] Terada T, Masuda S, Asaka J, Tsuda M, Katsura T, Inui K. Molecular cloning, functional characterization and tissue distribution of rat H^+/organic cation antiporter MATE1. Pharm Res 2006;23:1696–701.
[8] Masuda S, Terada T, Yonezawa A, Tanihara Y, Kishimoto K, Katsura T, et al. Identification and functional characterization of a new human kidney-specific H^+/organic cation antiporter, kidney-specific multidrug and toxin extrusion 2. J Am Soc Nephrol 2006;17:2127–35.
[9] Urakami Y, Nakamura N, Takahashi K, Okuda M, Saito H, Hashimoto Y, et al. Gender differences in expression of organic cation transporter OCT2 in rat kidney. FEBS Lett 1999;461:339–42.
[10] Urakami Y, Okuda M, Saito H, Inui K. Hormonal regulation of organic cation transporter OCT2 expression in rat kidney. FEBS Lett 2000;473:173–6.
[11] Ji L, Masuda S, Saito H, Inui K. Down-regulation of rat organic cation transporter rOCT2 by 5/6 nephrectomy. Kidney Int 2002;62:514–24.
[12] Yano I, Ito T, Takano M, Inui K. Evaluation of renal tubular secretion and reabsorption of levofloxacin in rats. Pharm Res 1997;14:508–11.
[13] Kaneniwa N, Funaki T, Furuta S, Watari N. High-performance liquid chromatographic determination of

cimetidine in rat plasma, urine and bile. J Chromatogr 1986;374:430–4.
[14] Masuda S, Saito H, Nonoguchi H, Tomita K, Inui K. mRNA distribution and membrane localization of the OAT-K1 organic anion transporter in rat renal tubules. FEBS Lett 1997;407:127–31.
[15] Urakami Y, Okuda M, Masuda S, Saito H, Inui K. Functional characteristics and membrane localization of rat multispecific organic cation transporters, OCT1 and OCT2, mediating tubular secretion of cationic drugs. J Pharmacol Exp Ther 1998;287:800–5.
[16] Takeuchi A, Masuda S, Saito H, Doi T, Inui K. Role of kidney-specific organic anion transporters in the urinary excretion of methotrexate. Kidney Int 2001;60:1058–68.
[17] Buist SC, Cherrington NJ, Choudhuri S, Hartley DP, Klaassen CD. Gender-specific and developmental influences on the expression of rat organic anion transporters. J Pharmacol Exp Ther 2002;301:145–51.
[18] Lu R, Kanai N, Bao Y, Wolkoff AW, Schuster VL. Regulation of renal oatp mRNA expression by testosterone. Am J Physiol 1996;270:F332–7.
[19] Kwon TH, Frokiaer J, Fernandez-Llama P, Maunsbach AB, Knepper MA, Nielsen S. Altered expression of Na transporters NHE-3, NaPi-II, Na-K-ATPase, BSC-1, and TSC in CRF rat kidneys. Am J Physiol 1999;277:F257–70.
[20] Hiasa M, Matsumoto T, Komatsu T, Moriyama Y. Wide variety of locations for rodent MATE1, a transporter protein that mediates the final excretion step for toxic organic cations. Am J Physiol Cell Physiol 2006;291:C678–86.
[21] Yonezawa A, Masuda S, Yokoo S, Katsura T, Inui K. Cisplatin and oxaliplatin, but not carboplatin and nedaplatin, are substrates for human organic cation transporters (SLC22A1-3 and multidrug and toxin extrusion family). J Pharmacol Exp Ther 2006;319:879–86.
[22] Kinsella JL, Aronson PS. Properties of the Na^+–H^+ exchanger in renal microvillus membrane vesicles. Am J Physiol 1980;238:F461–9.
[23] Takano M, Inui K, Okano T, Hori R. Cimetidine transport in rat renal brush border and basolateral membrane vesicles. Life Sci 1985;37:1579–85.
[24] Takano M, Inui K, Okano T, Saito H, Hori R. Carrier-mediated transport systems of tetraethylammonium in rat renal brush-border and basolateral membrane vesicles. Biochim Biophys Acta 1984;773:113–24.
[25] Aronson PS. Role of ion exchangers in mediating NaCl transport in the proximal tubule. Kidney Int 1996;49:1665–70.
[26] Moe OW. Acute regulation of proximal tubule apical membrane Na/H exchanger NHE-3: role of phosphorylation, protein trafficking, and regulatory factors. J Am Soc Nephrol 1999;10:2412–25.

balt5/zpt-pt/zpt-pt/zpt00507/zpt7458-07a | ironmong | S=6 | 3/16/07 | 11:58 | Art: 118695 | Input-jlt

0022-3565/07/3212-1–6$20.00
THE JOURNAL OF PHARMACOLOGY AND EXPERIMENTAL THERAPEUTICS
Copyright © 2007 by The American Society for Pharmacology and Experimental Therapeutics
JPET 321:1–6, 2007

Vol. 321, No. 2
118695/3202674
Printed in U.S.A.

Characterization of the Basal Promoter Element of Human Organic Cation Transporter 2 Gene

Jun-ichi Asaka, Tomohiro Terada, Ken Ogasawara, Toshiya Katsura, and Ken-ichi Inui

Department of Pharmacy, Kyoto University Hospital, Faculty of Medicine, Kyoto University, Kyoto, Japan

Received December 15, 2006; accepted February 20, 2007

ABSTRACT

Human organic cation transporter 2 (hOCT2; SLC22A2) is abundantly expressed in the kidney, and it plays important roles in the renal tubular secretion of cationic drugs. Although the transport characteristics of hOCT2 have been studied extensively, there is no information available for the transcriptional regulation of hOCT2. The present study was undertaken to identify the *cis*-element and *trans*-factor for basal expression of hOCT2. The transcription start site was located 385 nucleotides above the translation start site by using 5′-rapid amplification of cDNA ends. An approximately 4-kilobase fragment of the hOCT2 promoter region was isolated and the promoter activities were measured in the renal epithelial cell line LLC-PK_1. A deletion analysis suggested that the region spanning −91 to −58 base pairs was essential for basal transcriptional activity. This region lacked a TATA-box but contained a CCAAT box and an E-box. Electrophoretic mobility shift assays showed that specific DNA/protein complexes were present in the E-box but not in the CCAAT box, and supershift assays revealed that upstream stimulatory factor 1 (USF-1), which belongs to the basic helix-loop-helix-leucine zipper family of transcription factors, bound to the E-box. Mutation of the E-box resulted in a decrease in hOCT2 promoter activity, and overexpression of USF-1 enhanced the hOCT2 promoter activity in a dose-dependent manner. This article reports the first characterization of the hOCT2 promoter and shows that USF-1 functions as a basal transcriptional regulator of the hOCT2 gene via the E-box.

Numerous organic cations, including endogenous substances, xenobiotics, and metabolites, are excreted from the body. The kidney is critical for the elimination of organic cations, as is the liver, through active secretion via organic cation transport systems. The membrane potential-dependent organic cation transporters (OCTs) are located at the basolateral membrane of renal tubular cells, and they mediate the cellular uptake of cationic compounds from the blood (Koepsell, 1998; Inui et al., 2000; Jonker and Schinkel, 2004). In the brush-border membranes, organic cations are excreted via H^+/organic cation antiport systems, which have been recently identified by Otsuka et al. (2005) and ourselves (Masuda et al., 2006; Terada et al., 2006) as the part of multidrug and toxin extrusion family.

Human (h)OCT2 and hOCT3, but not hOCT1, are expressed in the kidney, and hOCT2 was found to be the most abundant organic cation transporter in the kidney (Motohashi et al., 2002). In addition, recent functional studies revealed that hOCT2 can transport several clinically important compounds such as creatinine (Urakami et al., 2002), the biguanide agent metformin (Kimura et al., 2005), and the anticancer agents cisplatin (Ciarimboli et al., 2005; Yonezawa et al., 2006) and oxaliplatin (Yonezawa et al., 2006). Drug-drug interaction between cetirizine, a new histamine H_1 blocker, and pilsicainide, a new type of antiarrhythmic drug, was also demonstrated to be mediated by OCT2 in patients with renal insufficiency (Tsuruoka et al., 2006).

So far, the pharmacokinetic significance of hOCT2 has been mainly demonstrated by expression and functional transport analyses. Regarding the regulatory aspects, transport activity of hOCT2 is controlled by protein phosphorylation, which is caused by protein kinase C, protein kinase A, phosphatidylinositol 3-kinase, and calcium/calmodulin complex, and the substrate affinity, plasma membrane expression of hOCT2, or both were altered (Çetinkaya et al., 2003; Biermann et al., 2006). In contrast, transcriptional mechanisms of the hOCT2 gene have not been elucidated. Among the human organic ion transporter family, hepatic expression of human organic anion transporter 2 (Popowski et al., 2005)

This work was supported in part by the 21st Century Center of Excellence (COE) program "Knowledge Information Infrastructure for Genome Science" and by a grant-in-aid for scientific research from the Ministry of Education, Culture, Sports, Science and Technology of Japan. J. A. is supported as a Research Assistant by the 21st Century COE program "Knowledge Information Infrastructure for Genome Science".

Article, publication date, and citation information can be found at http://jpet.aspetjournals.org.

doi:10.1124/jpet.106.118695.

ABBREVIATIONS: OCT, organic cation transporter; h, human; USF, upstream stimulatory factor; RACE, rapid amplification of cDNA ends; PCR, polymerase chain reaction; EMSA, electrophoretic mobility shift assay; HO, heme oxygenase; SNP, single-nucleotide polymorphism; rSNP, regulatory single-nucleotide polymorphism; WT, wild-type/wild type.

and hOCT1 (Saborowski et al., 2006) was shown to be *trans*-activated by the hepatocyte nuclear factor 4α and suppressed by bile acids via small heterodimer partner. In the kidney, it has been recently demonstrated that the promoter activity of human organic anion transporter 3 is regulated by hepatocyte nuclear factor 1α (Kikuchi et al., 2006), cAMP response element-binding protein-1, and activating transcription factor-1 (Ogasawara et al., 2006).

In the present study, to fully understand the basic transcriptional regulation of hOCT2, we cloned the 5′-flanking region of the hOCT2 gene and identified the minimal region necessary for basal promoter activity. The present results provide direct evidence for the involvement of upstream stimulatory factor (USF)-1, which belongs to the basic helix-loop-helix-leucine zipper family of transcription factors, bound to an E-box, in the regulation of basal promoter activity of hOCT2.

Materials and Methods

Materials. Restriction enzymes were obtained from New England Biolabs (Beverly, MA). T4 kinase and T4 DNA ligase were purchased from Takara Bio (Otsu, Japan). [γ-^{32}P]ATP was obtained from GE Healthcare (Little Chalfont, Buckinghamshire, UK). Antibodies used for supershift assays were purchased from Santa Cruz Biotechnology, Inc. (Santa Cruz, CA).

Determination of the Putative Transcription Start Site. The putative transcription start sites for hOCT2 were determined by 5′-rapid amplification of cDNA ends (5′-RACE) using Human Kidney Marathon-Ready cDNA (Clontech, Mountain View, CA) according to the manufacturer's instructions. The hOCT2 gene-specific primers for the RACE were designed and synthesized based on the genomic sequence. The 5′-RACE was performed with an adaptor primer 1, which came with the kit and a gene-specific primer of hOCT2. Nested PCR was performed with an adaptor primer 2 and a nested gene-specific primer of hOCT2 (primer sequences are shown in Table 1). The PCR products were subcloned into the pGEM-T Easy Vector (Promega, Madison, WI) and sequenced using a multicapillary DNA sequencer RISA384 system (Shimadzu, Kyoto, Japan). T1 AQ: C

Genomic Cloning of the hOCT2 Promoter. The hOCT2 promoter was isolated from the human genomic DNA (Promega) by a PCR-based method using primers designed based on the human genomic DNA (Table 1). The PCR product was isolated by electrophoresis and subcloned into the firefly luciferase reporter vector, pGL3-Basic (Promega), at KpnI and MluI sites. This full-length reporter plasmid is hereafter referred to as −4261/+23. The transcription factor-binding sites were predicted with TRANSFAC 6.0 software (http://www.gene-regulation.com/cgi-bin/pub/programs/match/bin/match.cgi?), with a core similarity of 0.95 and a matrix similarity of 0.90. AQ: D

Preparation of Deletion Reporter Constructs. The 5′-deleted constructs (−3654/+23, −3140/+23, −2479/+23, −1291/+23, −468/+23, and −411/+23) were generated by digestion of the −4261/+23 construct with KpnI and each of the following enzymes: EcoRI, BstXI, AatII, PstI, StuI, and NsiI, respectively. The ends were blunted with T4 DNA polymerase (Takara Bio) and then self-ligated. The other constructs were generated by PCR with primers containing a KpnI site and a MluI site (Table 1). The site-directed mutations in the putative E-box were introduced into the −91/+23 construct with a QuikChange II site-directed mutagenesis kit (Stratagene, La

TABLE 1
Oligonucleotide sequences of primers

Name	Sequence	Position
5′-RACE		NM_003058
GSP	5′-CGGCCAAACCTGTCTGCTATGTAGCCG-3′	697/671
NGSP	5′-TCCATGCTCCAGGACATCGTCCACGGT-3′	207/180
hOCT2 cloning		NT_007422.12
hOCT2 −4261	5′-GGGGTACCCAGGAGCCTTCATTCAGAATG-3′	−4261/−4239
hOCT2 −294	5′-GGGGTACCGACGGCTCTTGTTGTTGGTTG-3′	−294/−273
hOCT2 −150	5′-GGGGTACCATCCTAAGGCTCACGGCCAAC-3′	−150/−121
hOCT2 −91	5′-GGGGTACCGCCTTGTGGCCAAACACGTGT-3′	−91/−70
hOCT2 −58	5′-GGGGTACCGCCTTGAAGAAAAGCTGGCG-3′	−58/−39
hOCT2 −40	5′-GGGCTAGTTCTCCATAGGGCCTTGAAG-3′	−40/−19
hOCT2 −18	5′-GGGGTACCATTAAGTTCCTGGCTGCTCG-3′	−18/−3
hOCT2 +23	5′-CGACGCGTTCACAGCCCAGTAATCTTCCC-3′	1/23
USF-1 Cloning		NM_007122
Forward	5′-TCGGGAATTCCCCCTCACAGAGAGATGAAGGGG-3′	97/129
Reverse	5′-GATCCCTCGAGTTAGTTGCTGTCATTCTTGATGACG-3′	1029/1053
EMSA probe		
Collagen gene		Nagato et al. (2004)
Forward	5′-AAGAGATTAACCAATCACGTACGGTCT-3′	
Reverse	5′-AGACCGTACGTGATTGGTTAATCTCTT-3′	
Collagen mutCCAAT		Nagato et al. (2004)
Forward	5′-AAGAGATTAATCTAGCACGTACGGTCT-3′	
Reverse	5′-AGACCGTACGTGCTAGATTAATCTCTT-3′	
HO-1		Hock et al. (2004)
Forward	5′-GCCTTGTGGCCAAACACGTGTGTTTTCT-3′	
Reverse	5′-AGAAAACACAGCTGTTTGGCCACAAGGC-3′	
HO-1 mutECCAAT		
Forward	5′-GCCTTGTGGCCAAACATTTGTGTTTTCT-3′	
Reverse	5′-AGAAAACACAAATGTTTGGCCACAAGGC-3′	
hOCT2		NT_007422.12
Forward	5′-GCCTTGTGGCCAAACACGTGTGTTTTCT-3′	−101/−74
Reverse	5′-AGAAAACACACGTGTTTGGCCACAAGGC-3′	−101/−74
hOCT2 mutCCAAT		NT_007422.12
Forward	5′-GCCTTGTGGTCTAGCACGTGTGTTTTCT-3′	−101/−74
Reverse	5′-AGAAAACACACGTGCTAGACCACAAGGC-3′	−101/−74
hOCT2 mutE-box		NT_007422.12
Forward	5′-GCCTTGTGGCCAAACATTTGTGTTTTCT-3′	−101/−74
Reverse	5′-AGAAAACACAAATGTTTGGCCACAAGGC-3′	−101/−74

Jolla, CA) with the primers listed in Table 1. The nucleotide sequences of these deleted or mutated constructs were verified.

Cloning of hUSF-1 cDNA. cDNA for hUSF-1 (accession no. NM_007122) was isolated from Human Kidney Marathon-Ready cDNA (Clontech). Primers are listed in Table 1. The PCR product was subcloned into the expression vector pcDNA 3.1 (Invitrogen, Carlsbad, CA), and its sequence was verified.

Cell Culture and Luciferase Assay. The porcine kidney epithelial cell line LLC-PK_1 was obtained from American Type Culture Collection (ATCC CRL-1392; Manassas, VA). Cell culture, transfection, and the luciferase assay were performed as described previously (Asaka et al., 2006).

Electrophoretic Mobility Shift Assay. Nuclear extract was prepared from LLC-PK_1 cells according to the method of Shimakura et al. (2005). The probes listed in Table 1 were prepared by annealing complementary sense and antisense oligonucleotides, followed by end-labeling with [γ-^{32}P]ATP using T4 polynucleotide kinase (Takara Bio) and purification through a Sephadex G-25 column (GE Healthcare). The binding mixture consisted of 10 μg of LLC-PK_1 nuclear extract and unlabeled competitor probes in a buffer solution containing 120 mM KCl, 20 mM Tris-HCl, pH 7.5, 1.5 mM EDTA, 2 mM dithiothreitol, 10 mM NaF, 0.1 mM Na_3VO_4, 5% mM glycerol, 4% 3-[(3-cholamidopropyl)-dimethylammonio]-1-propanesulfonate, and 2% protease inhibitor cocktail (Nacalai Tesque, Kyoto, Japan). After preincubation for 30 min, labeled probes (~0.4 ng) were added, and the binding mixture was incubated for a further 30 min. For supershift assays, 1 μg of USF-1 antibody (sc-8983X) or USF-2 antibody (sc-862X) was added 30 min before the addition of the labeled probe. The volume of the binding mixture was 20 μl throughout the experiment. The DNA-protein complex was then separated on a 4% polyacrylamide gel at room temperature in 0.5× Tris borate-EDTA buffer. The gels were dried and exposed to X-ray film for autoradiography.

Data Analysis. The results were expressed relative to the pGL3-Basic vector set, and they represent the means ± S.E. of three replicates. Two or three experiments were conducted, and representative results are shown. Data were analyzed statically by the Student's *t* test or by the one-way analysis of variance followed by Dunnett's test.

Results

Determination of the Transcription Start Site for hOCT2 in Human Kidney Using 5′-RACE. The transcription start site for hOCT2 in the human kidney was identified by 5′-RACE. The putative start site was determined using the longest RACE product. Sequencing of the amplified bands revealed that the terminal position of hOCT2 cDNA with the longest 5′-untranslated region was located 385 nucleotides above the translation start site, which is 243 base pairs upstream of the 5′-end of hOCT2 cDNA reported previously (Gorboulev et al., 1997). So, the terminal position of hOCT2 cDNA with the longest 5′-untranslated region was numbered +1 as the transcription start site in this study.

Isolation and Analysis of the 5′-Flanking Region of the hOCT2 Gene. Based on the result of 5′-RACE, approximately 4 kilobases of the 5′-flanking region of the hOCT2 gene were isolated and subcloned into pGL3-Basic. Promoter activity was assessed in LLC-PK_1 cells, because this cell line has active organic cation transport systems (Saito et al., 1992), and it shows promoter activity of rat OCT2 (Asaka et al., 2006). To determine the minimal region required for basal activity of the promoter, a series of deletion constructs were transfected into LLC-PK_1 cells, and luciferase activity was measured (Fig. 1). The longest reporter construct

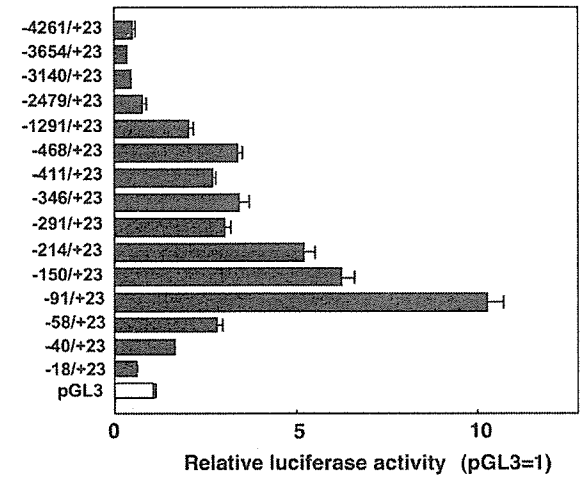

Fig. 1. Identification of transcriptional activity and deletion analysis of the hOCT2 promoter in LLC-PK_1 cells. A series of deleted promoter constructs [equimolar amounts of the −4261/+23 construct (600 ng)] were transfected into LLC-PK_1 cells for luciferase assays. Firefly luciferase activity was normalized to *Renilla* luciferase activity. Data are reported as the relative -fold increase compared with pGL3-Basic vector and represent the means ± S.E. of three replicates. This figure is a representative one from three separate experiments.

(−4261/+23) had the same level of luciferase activity as the control vector pGL3-Basic. The level of luciferase activity gradually increased as the region spanning from −4261 to −91 was deleted, and the reporter construct (−91/+23) had approximately 10-fold more luciferase activity than pGL3-Basic. In contrast, the constructs (−58/+23, −40/+23, and −18/+23) exhibited little luciferase activity. These results suggested that the region between −91 and −58 contained positive *cis*-acting elements for efficient basal expression of the hOCT2 gene. Figure 2 shows a computational analysis of the −106/−58 region of the hOCT2 promoter. Using TRANSFAC 6.0 (www.gene-regulation.com/), we found a putative CCAAT box (5′-CCAAA-3′) and E-box (5′-CACGTG-3′) in this region. The CCAAT box can be recognized by several transcription factors such as CCAAT/enhancer-binding proteins (Ramji and Foka, 2002) and nuclear factor-Y (Mantovani, 1999), and the E-box is stimulated by USFs (Corre and Galibert, 2005). These transcription factors were reported to help maintain the basal promoter activities of various genes.

Electrophoretic Mobility Shift Assay. To confirm which *cis*-element was involved in the basal promoter activity, EMSA was performed using nuclear extract from LLC-PK_1 cells and the hOCT2 probe (−101/−74), which contains both a CCAAT box and an E-box. At first, we tested the involvement of the CCAAT box. For a positive control of the

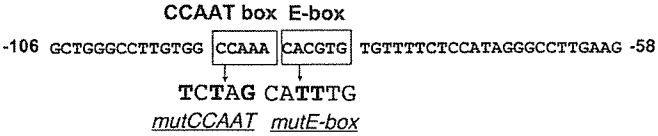

Fig. 2. Nucleotide sequence of the promoter region (−106 to −58) that had the highest level of basal activity. Numbering is relative to the transcription start site. Putative binding sites for the transcription factors are indicated on the sequence. Site-directed mutations that destroy putative transcription factor-binding elements were introduced individually and designated *mutCCAAT* and *mut E-box*. The nucleotides altered for the mutational analysis are shown in bold under the wild-type (WT) sequence.

EMSA for the CCAAT box, an oligonucleotide of the CCAAT box derived from the human pro-α3(V) collagen gene (Nagato et al., 2004) was used. As shown in Fig. 3, a specific DNA-protein complex was observed using the pro-α3(V) collagen gene CCAAT box probe (lane 2). In the same buffer, the hOCT2 (−101/−74) probe formed a DNA-protein complex (lane 6), but this was prevented by the hOCT2 probe with mutCCAAT, which lacks a CCAAT box (lane 8). Furthermore, the consensus sequence for the CCAAT box did not prevent the formation of the complex (lane 9). These results suggested that nuclear extracts did not bind to the CCAAT box.

We then examined the contribution of the E-box. For a positive control, a oligonucleotide for the E-box derived from the heme oxygenase (HO)-1 promoter (Hock et al., 2004) was used. As shown in Fig. 4, a specific DNA-protein complex was observed using the HO-1 gene E-box probe (lane 2), and this complex was supershifted using anti USF-1 antibody (lane 3). In these conditions, the hOCT2 probe also formed a DNA-protein complex (lane 6). The formation of this complex was completely prevented by the addition of an excess amount of unlabeled oligonucleotide for the hOCT2 probe (lane 7), hOCT2 mutCCAAT (lane 9), and the consensus sequence for the E-box (lane 10), but not by mutE-box lacking an E-box (lane 8). Furthermore, anti-USF-1 antibody, but not anti USF-2 antibody, was able to supershift the DNA-protein complex (lanes 11 and 12). These results indicated that USF-1 bound to the E-box of the hOCT2 promoter.

Mutagenesis of the E-box. To confirm the functional importance of the E-box, mutations were introduced into the −150/+23 and −91/+23 constructs and their promoter activities were examined. As shown in Fig. 5, both constructs lost all luciferase activity compared with the wild type. These results suggest that the E-box is responsible for the basal promoter activity of hOCT2.

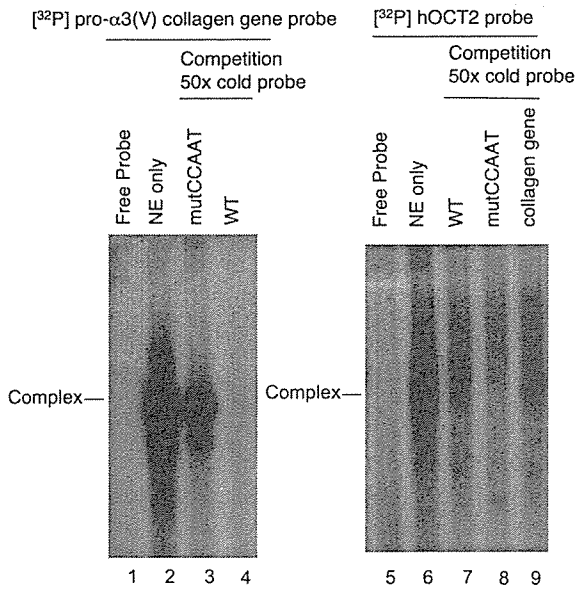

Fig. 3. EMSA of LLC-PK$_1$ nuclear proteins binding to the probes containing putative CCAAT box-binding elements. Nuclear extract from LLC-PK$_1$ cells was incubated with the ^{32}P-labeled oligonucleotide probes [pro 3α(V) collagen gene probe and hOCT2 probe] alone (lanes 2 and 6) or in the presence of excess unlabeled WT oligonucleotide (lanes 4 and 7), mutated oligonucleotide (lanes 3 and 8), or pro 3α(V) collagen gene oligonucleotide (lane 9). In lanes 1 and 5, nuclear extract was not added.

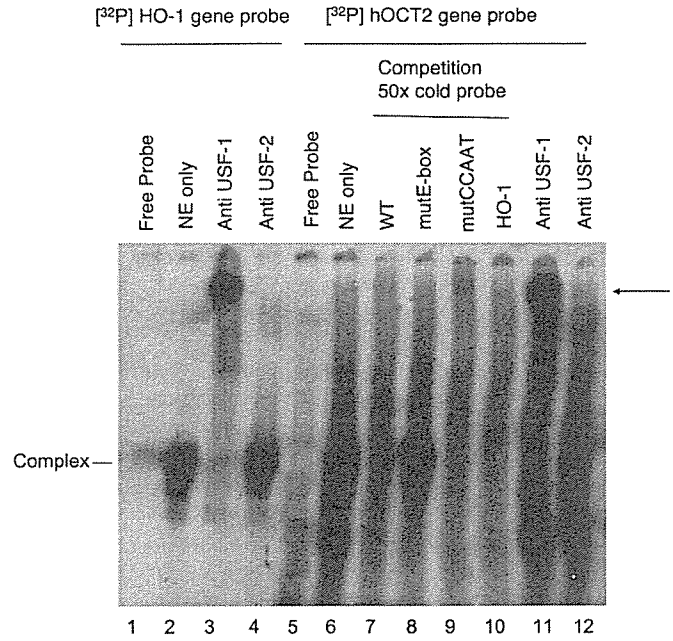

Fig. 4. EMSA of LLC-PK$_1$ nuclear proteins binding to the probes containing putative E-box binding elements. Nuclear extract from LLC-PK$_1$ cells was incubated with the ^{32}P-labeled oligonucleotide probes (heme oxygenase-1 gene probe and hOCT2 probe) alone (lanes 2 and 6) or in the presence of excess unlabeled WT oligonucleotide (lane 7), E-box mutated oligonucleotide (lane 8), CCAAT box mutated oligonucleotide (lane 9), HO-1 gene oligonucleotide (lane 10), anti USF-1 antibody (lanes 3 and 11), and anti USF-2 antibody (lanes 4 and 12). In lanes 1 and 5, nuclear extract was not added. An arrow indicates the supershifted complexes.

Transactivation of the Promoter Activity by Overexpression of USF-1. Finally, we investigated the effect of the overexpression of USF-1 on the promoter activity of hOCT2 (Fig. 6). The −91/+23 construct was cotransfected into LLC-PK$_1$ cells with the USF-1 expression vector. The promoter activity of hOCT2 showed a dose-dependent increase on the coexpression of USF-1, providing direct evidence that USF-1 enhanced the promoter activity.

Discussion

In the present study, we performed a functional promoter assay of hOCT2, and we obtained convincing evidence of the involvement of USF-1 bound to an E-box in the regulation of hOCT2 basal expression. This conclusion is supported by results of experiments involving EMSAs, mutagenesis of the E-box, and overexpression of USF-1. USF-1 was originally described as a transcription factor derived from HeLa nuclear extract that binds to an E-box of the adenovirus major late promoter (Sawadogo and Roeder, 1985). Subsequent analysis revealed that this factor is involved in the basal transcriptional regulation of various genes, including the human angiotensinogen (Yanai et al., 1997), HO-1 (Hock et al., 2004), and prolyl-4-hydroxylase (I) (Chen et al., 2006) genes. Furthermore, USF acts not only as a classical upstream activator but also as a factor that interacts with initiator elements of a variety of core promoters, which can lead to markedly enhanced levels of basal transcription (Corre and Galibert, 2005). The core E-box sequence CANNTG is usually conserved, with the two central sequence nucleotides (NN), in most cases, either GC or CG (Corre and Galibert, 2005). Because the E-box of hOCT2 is

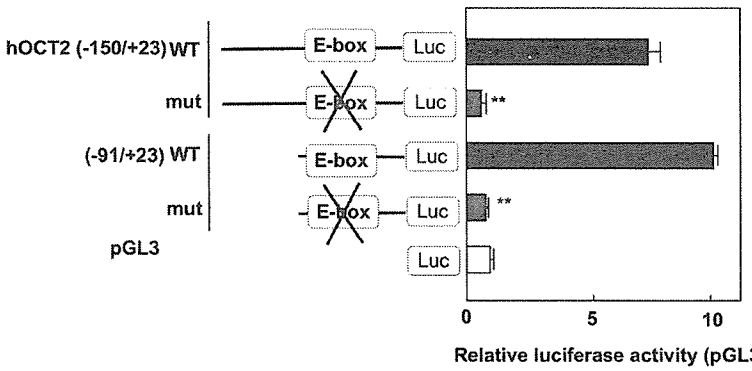

Fig. 5. Mutational analysis of the putative E-box binding elements of the hOCT2 promoter. The mutated −150/+23 and −91/+23 constructs (600 ng) were transiently expressed in LLC-PK$_1$ cells for luciferase assays. Firefly luciferase activity was normalized to *Renilla* luciferase activity. Data are reported as the relative -fold increase compared with pGL3-Basic vector and represent the means ± S.E. of three replicates. **, $P < 0.01$, significantly different from WT. This figure is a representative one from three separate experiments.

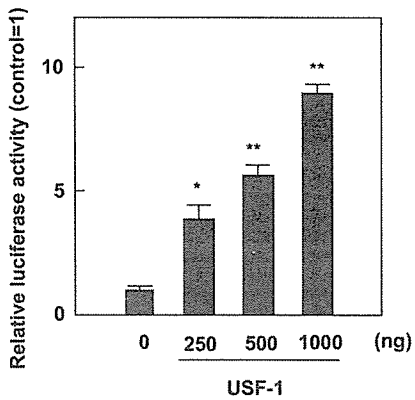

Fig. 6. Effect of hUSF-1 overexpression on hOCT2 transcriptional activity. LLC-PK$_1$ cells were transiently transfected with 250 ng of the −91/+23 construct and 250, 500, and 1000 ng of the hUSF-1 expression vector. The total amount of transfected DNA was kept constant by adding empty vector. Data are reported as the relative -fold increase compared with no hUSF-1 and represent the means ± S.E. of three replicates. *, $P < 0.05$, significantly different from control (no USF-1. **, $P < 0.01$, significantly different from control. This figure is a representative one from three separate experiments.

CACGTG, a perfectly conserved consensus sequence, it is also reasonable that USF-1 binds to the E-box of the hOCT2 promoter region.

USF-1 is a key regulator of a number of gene regulatory networks, including the stress and immune responses, cell cycle and proliferation, and lipid and glucid metabolism (Corre and Galibert, 2005). Familial combined hyperlipidemia, characterized by elevated levels of serum total cholesterol, triglycerides, or both, is associated with the USF-1 haplotype (Pajukanta et al., 2004). Recently, it was reported that USF-1 gene polymorphisms are associated with increased sensitivity to antilipolytic insulin (Kantartzis et al., 2007). In human kidney, the mRNA level of hOCT2 was highest of any of the OCT family (Motohashi et al., 2002), suggesting that hOCT2 has a more important role in the transport of organic cations across the basolateral membrane than other members of the hOCT family in the proximal tubules. However, the expression pattern of renal drug transporters was reported to vary among patients (Terada and Inui, 2007). This variation may be caused by single-nucleotide polymorphisms (SNPs) in the hOCT2 promoter region or USF-1 coding region.

Regulatory SNPs (rSNPs), which lie outside of the amino acid coding regions of genes, affect the regulation of gene expression. Recent research suggests that approximately 50% of genes have one or more common rSNPs associated with gene expression (Buckland, 2006). For example, the uridine diphosphate glucuronosyltransferase UGT1A1*28 polymorphism, characterized by an extra TA repeat in the promoter region of the gene, is involved in the toxicity of irinotecan (Iyer et al., 2002). Thiopurine *S*-methyltransferase, which is required to metabolize thiopurine, has a variable number tandem repeats in the 5′-flanking region involved in the gene expression (Alves et al., 2001). In addition, it has been reported that a rSNP of *SLC22A5* (*OCTN2*) affects the transcription of OCTN2, contributing to the pathogenesis of Crohn's disease (Peltekova et al., 2004). A rSNP within the E-box core motif also modulates gene regulation. For example, a single base transition within the USF E-box consensus sequence of the thymidylate synthase gene, implicated in the metabolism of folate, prevents the USF complex from binding to its cognate sequence (Mandola et al., 2003). It is unknown whether SNPs exist in the hOCT2 gene E-box, but it is possible that these SNPs affect the pharmacokinetics of cationic drugs.

USF-1 is a ubiquitously expressed transcription factor (Sirito et al., 1994), but hOCT2 is mainly expressed in the kidney (Urakami et al., 2002). The mechanism of this tissue-specific expression has not been clarified yet. The E-box of the hibernation-specific protein HP-27 is hypomethylated in the liver, but it is highly methylated in the kidney and heart, being involved in liver-specific expression (Fujii et al., 2006). Kidney-specific transcription may be controlled by methylation of the E-box in the kidney or an unidentified kidney-specific transcription factor.

In conclusion, the present results indicate that USF-1 functions as a basal transcriptional regulator of the hOCT2 gene, making this study the first to identify the *cis*-elements and *trans*-factors necessary for the regulation of hOCT2. These findings should serve as a basis for future investigations into the molecular regulation of the transport of organic cations and some pharmaceuticals in the human kidney.

References

Alves S, Amorim A, Ferreira F, and Prata MJ (2001) Influence of the variable number of tandem repeats located in the promoter region of the thiopurine methyltransferase gene on enzymatic activity. *Clin Pharmacol Ther* **70**:165–174.

Asaka J, Terada T, Okuda M, Katsura T, and Inui K (2006) Androgen receptor is responsible for rat organic cation transporter 2 gene regulation but not for rOCT1 and rOCT3. *Pharm Res (NY)* **23**:697–704.

Biermann J, Lang D, Gorboulev V, Koepsell H, Sindic A, Schröter R, Zvirbliene A, Pavenstädt H, Schlatter E, and Ciarimboli G (2006) Characterization of regulatory mechanisms and states of human organic cation transporter 2. *Am J Physiol* **290**:C1521–C1531.

Buckland PR (2006) The importance and identification of regulatory polymorphisms and their mechanisms of action. *Biochim Biophys Acta* **1762**:17–28.

Çetinkaya I, Ciarimboli G, Yalçinkaya G, Mehrens T, Velic A, Hirsch JR, Gorboulev V, Koepsell H, and Schlatter E (2003) Regulation of human organic cation trans-

porter hOCT2 by PKA, PI3K, and calmodulin-dependent kinase. *Am J Physiol* **284:**F293–F302.

Chen L, Shen YH, Wang X, Wang J, Gan Y, Chen N, Wang J, LeMaire SA, Coselli JS, and Wang XL (2006) Human prolyl-4-hydroxylase α(I) transcription is mediated by upstream stimulatory factors. *J Biol Chem* **281:**10849–10855.

Ciarimboli G, Ludwig T, Lang D, Pavenstädt H, Koepsell H, Piechota HJ, Haier J, Jaehde U, Zisowsky J, and Schlatter E (2005) Cisplatin nephrotoxicity is critically mediated via the human organic cation transporter 2. *Am J Pathol* **167:**1477–1484.

Corre S and Galibert MD (2005) Upstream stimulating factors: highly versatile stress-responsive transcription factors. *Pigment Cell Res* **18:**337–348.

Fujii G, Nakamura Y, Tsukamoto D, Ito M, Shiba T, and Takamatsu N (2006) CpG methylation at the USF-binding site is important for the liver-specific transcription of the chipmunk HP-27 gene. *Biochem J* **395:**203–209.

Gorboulev V, Ulzheimer JC, Akhoundova A, Ulzheimer-Teuber I, Karbach U, Quester S, Baumann C, Lang F, Busch AE, and Koepsell H (1997) Cloning and characterization of two human polyspecific organic cation transporters. *DNA Cell Biol* **16:**871–881.

Hock TD, Nick HS, and Agarwal A (2004) Upstream stimulatory factors, USF1 and USF2, bind to the human haem oxygenase-1 proximal promoter in vivo and regulate its transcription. *Biochem J* **383:**209–218.

Inui K, Masuda S, and Saito H (2000) Cellular and molecular aspects of drug transport in the kidney. *Kidney Int* **58:**944–958.

Iyer L, Das S, Janisch L, Wen M, Ramirez J, Karrison T, Fleming GF, Vokes EE, Schilsky RL, and Ratain MJ (2002) UGT1A1*28 polymorphism as a determinant of irinotecan disposition and toxicity. *Pharmacogenomics J* **2:**43–47.

Jonker JW and Schinkel AH (2004) Pharmacological and physiological functions of the polyspecific organic cation transporters: OCT1, 2, and 3 (SLC22A1-3). *J Pharmacol Exp Ther* **308:**2–9.

Kantartzis K, Fritsche A, Machicao F, Stumvoll M, Machann J, Schick F, Häring HU, and Stefan N (2007) Upstream transcription factor 1 gene polymorphisms are associated with high antilipolytic insulin sensitivity and show gene-gene interactions. *J Mol Med* **85:**55–61.

Kikuchi R, Kusuhara H, Hattori N, Shiota K, Kim I, Gonzalez FJ, and Sugiyama Y (2006) Regulation of the expression of human organic anion transporter 3 by hepatocyte nuclear factor 1 α/β and DNA methylation. *Mol Pharmacol* **70:**887–896.

Kimura N, Okuda M, and Inui K (2005) Metformin transport by renal basolateral organic cation transporter hOCT2. *Pharm Res (NY)* **22:**255–259.

Koepsell H (1998) Organic cation transporters in intestine, kidney, liver, and brain. *Annu Rev Physiol* **60:**243–266.

Mandola MV, Stoehlmacher J, Muller-Weeks S, Cesarone G, Yu MC, Lenz HJ, and Ladner RD (2003) A novel single nucleotide polymorphism within the 5′ tandem repeat polymorphism of the thymidylate synthase gene abolishes USF-1 binding and alters transcriptional activity. *Cancer Res* **63:**2898–2904.

Mantovani R (1999) The molecular biology of the CCAAT-binding factor NF-Y. *Gene (Amst)* **239:**15–27.

Masuda S, Terada T, Yonezawa A, Tanihara Y, Kishimoto K, Katsura T, Ogawa O, and Inui K (2006) Identification and functional characterization of a new human kidney-specific H^+/organic cation antiporter, kidney-specific multidrug and toxin extrusion 2. *J Am Soc Nephrol* **17:**2127–2135.

Motohashi H, Sakurai Y, Saito H, Masuda S, Urakami Y, Goto M, Fukatsu A, Ogawa O, and Inui K (2002) Gene expression levels and immunolocalization of organic ion transporters in the human kidney. *J Am Soc Nephrol* **13:**866–874.

Nagato H, Matsuo N, Sumiyoshi H, Sakata-Takatani K, Nasu M, and Yoshioka H (2004) The transcription factor CCAAT-binding factor CBF/NF-Y and two repressors regulate the core promoter of the human pro-α3(V) collagen gene (COL5A3). *J Biol Chem* **279:**46373–46383.

Ogasawara K, Terada T, Asaka J, Katsura T, and Inui K (2006) Human organic anion transporter 3 gene is regulated constitutively and inducibly via a cAMP-response element. *J Pharmacol Exp Ther* **319:**317–322.

Otsuka M, Matsumoto T, Morimoto R, Arioka S, Omote H, and Moriyama Y (2005) A human transporter protein that mediates the final excretion step for toxic organic cations. *Proc Natl Acad Sci USA* **102:**17923–17928.

Pajukanta P, Lilja HE, Sinsheimer JS, Cantor RM, Lusis AJ, Gentile M, Duan XJ, Soro-Paavonen A, Naukkarinen J, Saarela J, et al. (2004) Familial combined hyperlipidemia is associated with upstream transcription factor 1 (USF1). *Nat Genet* **36:**371–376.

Peltekova VD, Wintle RF, Rubin LA, Amos CI, Huang Q, Gu X, Newman B, Van Oene M, Cascon D, Greenberg G, et al. (2004) Functional variants of OCTN cation transporter genes are associated with Crohn disease. *Nat Genet* **36:**471–475.

Popowski K, Eloranta JJ, Saborowski M, Fried M, Meier PJ, and Kullak-Ublick GA (2005) The human organic anion transporter 2 gene is transactivated by hepatocyte nuclear factor-4α and suppressed by bile acids. *Mol Pharmacol* **67:**1629–1638.

Ramji DP and Foka P (2002) CCAAT/enhancer-binding proteins: structure, function and regulation. *Biochem J* **365:**561–575.

Saborowski M, Kullak-Ublick GA, and Eloranta JJ (2006) The human organic cation transporter-1 gene is transactivated by hepatocyte nuclear factor-4α. *J Pharmacol Exp Ther* **317:**778–785.

Saito H, Yamamoto M, Inui K, and Hori R (1992) Transcellular transport of organic cation across monolayers of kidney epithelial cell line LLC-PK_1. *Am J Physiol* **262:**C59–C66.

Sawadogo M and Roeder RG (1985) Interaction of a gene-specific transcription factor with the adenovirus major late promoter upstream of the TATA box region. *Cell* **43:**165–175.

Shimakura J, Terada T, Katsura T, and Inui K (2005) Characterization of the human peptide transporter PEPT1 promoter: Sp1 functions as a basal transcriptional regulator of human PEPT1. *Am J Physiol* **289:**G471–G477.

Sirito M, Lin Q, Maity T, and Sawadogo M (1994) Ubiquitous expression of the 43- and 44-kDa forms of transcription factor USF in mammalian cells. *Nucleic Acids Res* **22:**427–433.

Terada T and Inui K (2007) Gene expression and regulation of drug transporters in the intestine and kidney. *Biochem Pharmacol* **73:**440–449.

Terada T, Masuda S, Asaka J, Tsuda M, Katsura T, and Inui K (2006) Molecular cloning, functional characterization and tissue distribution of rat H^+/organic cation antiporter MATE1. *Pharm Res (NY)* **23:**1696–1701.

Tsuruoka S, Ioka T, Wakaumi M, Sakamoto K, Ookami H, and Fujimura A (2006) Severe arrhythmia as a result of the interaction of cetirizine and pilsicainide in a patient with renal insufficiency: first case presentation showing competition for excretion via renal multidrug resistance protein 1 and organic cation transporter 2. *Clin Pharmacol Ther* **79:**389–396.

Urakami Y, Akazawa M, Saito H, Okuda M, and Inui K (2002) cDNA cloning, functional characterization, and tissue distribution of an alternatively spliced variant of organic cation transporter hOCT2 predominantly expressed in the human kidney. *J Am Soc Nephrol* **13:**1703–1710.

Yanai K, Saito T, Hirota K, Kobayashi H, Murakami K, and Fukamizu A (1997) Molecular variation of the human angiotensinogen core promoter element located between the TATA box and transcription initiation site affects its transcriptional activity. *J Biol Chem* **272:**30558–30562.

Yonezawa A, Masuda S, Yokoo S, Katsura T, and Inui K (2006) Cisplatin and oxaliplatin, but not carboplatin and nedaplatin, are substrates for human organic cation transporters (SLC22A1–3 and multidrug and toxin extrusion family). *J Pharmacol Exp Ther* **319:**879–886.

Address correspondence to: Dr. Ken-ichi Inui, Department of Pharmacy, Kyoto University Hospital, Sakyo-ku, Kyoto 606-8507, Japan. E-mail: inui@kuhp.kyoto-u.ac.jp

balt5/zmo-mol/zmo-mol/zmo00607/zmo5162-07a	ironmong	S=5	3/19/07	10:09	4/Color Figure(s): 6	Art: 032938	Input-kag

0026-895X/07/7106-1–7$20.00
MOLECULAR PHARMACOLOGY

Mol Pharmacol 71:1–7, 2007

Vol. 71, No. 6
32938/3204758
Printed in U.S.A.

Identification of Essential Histidine and Cysteine Residues of H^+/Organic Cation Antiporter, Multidrug, and Toxin Extrusion[S]

Jun-ichi Asaka, Tomohiro Terada, Masahiro Tsuda, Toshiya Katsura, and Ken-ichi Inui

Department of Pharmacy, Kyoto University Hospital, Faculty of Medicine, Kyoto University, Sakyo-ku, Kyoto, Japan

Received November 22, 2006; accepted February 27, 2007

ABSTRACT

Multidrug and toxin extrusion 1 (MATE1) has been isolated as an H^+/organic cation antiporter located at the renal brush-border membranes. Previous studies using rat renal brush-border membrane vesicles indicated that cysteine and histidine residues played critical roles in H^+/organic cation antiport activity. In the present study, essential histidine and cysteine residues of MATE1 family were elucidated. When 7 histidine and 12 cysteine residues of rat (r)MATE1 conserved among species were mutated, substitution of His-385, Cys-62, and Cys-126 led to a significant loss of tetraethylammonium (TEA) transport activity. Cell surface biotinylation and immunofluorescence analyses with confocal microscopy indicated that rMATE1 mutant proteins were localized at plasma membranes. Mutation of the corresponding residues in human (h)MATE1 and hMATE2-K also diminished the transport activity. The transport of TEA via rMATE1 was inhibited by the sulfhydryl reagent *p*-chloromercuribenzenesulfonate (PCMBS) and the histidine residue modifier diethyl pyrocarbonate (DEPC) in a concentration-dependent manner. The PCMBS-caused inhibition of the transport via rMATE1 was protected by an excess of various organic cations such as TEA, suggesting that cysteine residues act as substrate-binding sites. In the case of DEPC, no such protective effects were observed. These results suggest that histidine and cysteine residues are required for MATE1 to function and that cysteine residues may serve as substrate-recognition sites.

Fabb

Proximal tubules play important roles in the renal elimination of drugs. Cationic drugs are secreted from blood to urine by the combined efforts of two distinct classes of organic cation transporters: one driven by the transmembrane electrical potential difference in the basolateral membranes, and the other driven by the transmembrane H^+ gradient in the brush-border membranes (Inui and Okuda, 1998). To date, three kinds of membrane potential-dependent organic cation transporters (OCT1~3) have been identified and characterized (Burckhardt and Wolff, 2000; Inui et al., 2000; Wright, 2005).

In contrast to OCTs, the molecular nature of H^+/organic cation antiport system has not been characterized, but recently, orthologs of the multidrug and toxin extrusion (MATE) family have been identified in various species (Otsuka et al., 2005a; Hiasa et al., 2006; Masuda et al., 2006; Terada et al., 2006). We have cloned rat (r)MATE1 cDNA and demonstrated that rMATE1 mRNA is mainly expressed in the kidney (proximal convoluted and straight tubules), and rMATE1 can transport not only organic cations such as tetraethylammonium (TEA), cimetidine, and metformin but also the zwitterionic compound cephalexin (Terada et al., 2006). Furthermore, we revealed recently that an oppositely directed H^+ gradient serves as a driving force for the transport of TEA via rMATE1 (Tsuda et al., 2007). We also cloned human (h)MATE2-K cDNA and revealed that hMATE2-K and the hMATE1 was localized at the brush-border membranes of renal proximal tubules (Masuda et al., 2006). hMATE2-K can also transport organic cations such as TEA, procainamide, metformin, and creatinine and works as an H^+/organic cation antiporter (Masuda et al., 2006). These studies suggested that the mammalian MATE family showed similar characteristics to the renal H^+/organic cation antiport system (Inui and Okuda, 1998; Wright, 2005). During the course of studying the transport of TEA using rat renal brush-border membrane vesicles, we found that treatment of membrane vesicles with sulfhydryl reagents such as *p*-chloromercuribenzenesulfonate (PCMBS) (Hori et al., 1987) and

This work was supported in part by the 21st Century Center of Excellence (COE) program "Knowledge Information Infrastructure for Genome Science," a Grant-in-Aid for Scientific Research from the Ministry of Education, Culture, Sports, Science and Technology of Japan, and a Grant-in-Aid for Research on Advanced Medical Technology from the Ministry of Health, Labor and Welfare of Japan. J.A. is supported as a Research Assistant by the 21st Century COE program "Knowledge Information Infrastructure for Genome Science."

Article, publication date, and citation information can be found at http://molpharm.aspetjournals.org.

doi:10.1124/mol.106.032938.

[S] The online version of this article (available at http://molpharm.aspetjournals.org) contains supplemental material.

ABBREVIATIONS: MATE, multidrug and toxin extrusion; TEA, tetraethylammonium; DEPC, diethyl pyrocarbonate; PCMBS, *p*-chloromercuribenzenesulfonate; OCT, organic cation transporter; PAH, *p*-aminohippurate; TBS, Tris-buffered saline; HEK, human embryonic kidney.

the histidine residue modifier diethyl pyrocarbonate (DEPC) (Hori et al., 1989) significantly inhibited [^{14}C]TEA transport by H^+/organic cation antiport system. Furthermore, very recently, Ohta et al. (2006) demonstrated that PCMBS inhibited the uptake of TEA by rMATE1. Based on these findings, it was speculated that histidine and cysteine residues play important roles in the transport activity of MATE family. The present study was undertaken to identify the essential histidine and cysteine residues of the MATE family (especially rMATE1) using site-directed mutagenesis and to examine their functional roles using chemical modifiers.

Materials and Methods

Materials. Cephalexin was donated by Shionogi Co. (Osaka, Japan). [^{14}C]TEA (2.035 GBq/mmol) was obtained from American Radiolabeled Chemicals Inc. (St. Louis, MO). DEPC, cimetidine, and TEA were obtained from Nacalai Tesque (Kyoto, Japan). PCMBS, metformin, and *p*-aminohippurate (PAH) were purchased from Sigma (St. Louis, MO). All other chemicals used were of the highest purity available.

Plasmids and Site-Directed Mutagenesis. The rMATE1 cDNA was excised from rMATE1/pcDNA3.1 (Terada et al., 2006), and was subcloned into pFLAG-CMV-6 (Sigma) to yield FLAG-rMATE1. The site-directed mutations of histidine or cysteine residues were introduced into FLAG-rMATE1, hMATE1/pcDNA3.1 (Yonezawa et al., 2006), or hMATE2-K/pcDNA3.1 (Masuda et al., 2006) with a QuikChange II site-directed mutagenesis kit (Stratagene, La Jolla, CA) with the primers listed in Supplemental Table S1. The nucleotide sequences of these constructs were confirmed using multicapillary DNA sequencer RISA384 system (Shimadzu, Kyoto, Japan).

Cell Culture, Transfection, and Transport Measurements. HEK293 cells (CRL-1573; American Type Culture Collection, Manassas, VA) were cultured as described previously (Urakami et al., 2002; Terada et al., 2006). Various constructs were transfected into HEK293 cells using LipofectAMINE 2000 Reagent (Invitrogen, Carlsbad, CA) according to the manufacturer's instructions. At 48 h after the transfection, the cells were used for uptake experiments. Cellular uptake of [^{14}C]TEA was measured with monolayers grown on poly(D-lysine)-coated 24-well plates. To manipulate the intracellular pH, intracellular acidification was performed by pretreatment with ammonium chloride (30 mM, 20 min at 37°C, pH 7.4) (Masuda et al., 2006; Terada et al., 2006). The medium was then removed, and 0.2 ml of incubation medium, pH 7.4, containing [^{14}C]TEA was added. The medium was aspirated off at the end of the incubation, and monolayers were rapidly rinsed twice with 1 ml of ice-cold incubation medium. The cells were solubilized in 0.5 ml of 0.5 N NaOH, and then the radioactivity in aliquots was determined by liquid scintillation counting. The protein content of the solubilized cells was determined using a Bio-Rad Protein Assay Kit (Bio-Rad Laboratories, Hercules, CA) with bovine γ-globulin as a standard.

Pretreatment with DEPC and PCMBS. HEK293 cells were washed twice with incubation medium, pH 7.4. Monolayers were then incubated with DEPC, pH 6.0, in phosphate-buffered saline for 10 min at 25°C or PCMBS, pH 7.4, in incubation medium for 10 min at 25°C. Then cells were washed twice before intracellular acidification.

Cell Surface Biotinylation. Cell surface biotinylation was performed according to the methods of Hong et al. (2004) with some modification. HEK293 cells were grown on poly(D-lysine)-coated six-well plates and transfected with the rMATE1cDNAs. At 48 h after the transfection, cells were washed with ice-cold phosphate-buffered saline calcium/magnesium (138 mM $NaCl_2$, 2.7 mM KCl, 1.5 mM KH_2PO_4, 9.6 mM Na_2HPO_4, 1 mM $MgCl_2$, and 0.1 mM $CaCl_2$, pH 7.3) and then treated with 1 ml of membrane-impermeable biotinylating agent, sulfo-NHS-SS-biotin (Pierce, Rockford, IL) (1.5 mg/ml) at 4°C for 1 h. Subsequently, the cells were washed three times with ice-cold phosphate-buffered saline calcium/magnesium containing 100 mM glycine and then incubated for 20 min at 4°C with the same buffer to remove the remaining labeling agent. After washing with phosphate-buffered saline calcium/magnesium, cells were disrupted with 700 μl of lysis buffer (10 mM Tris-base, 150 mM NaCl, 1 mM EDTA, 0.1% SDS, and 1% Triton X-100, pH 7.4) containing protease inhibitors at 4°C for 1 h with constant agitation. After centrifugation, 140 μl of streptavidin agarose beads (Pierce) were added to 600 μl of cell lysate and incubated for 1 h at room temperature to isolate the plasma membrane protein.

Western Blot Analysis. The procedures for Western blot analysis were described previously (Terada et al., 1996). Monoclonal anti-FLAG-M2 antibody (1:4000 dilution; Sigma) or Na^+/K^+-ATPase antibody (1:2000 dilution; Upstate Biotechnology, Lake Placid, NY) was used as the primary antibody. A peroxidase-conjugated anti-mouse IgG antibody was used for detection of bound antibodies, and strips of the blots were visualized by chemiluminescence on X-ray film.

Immunofluorescence of Transfected Cells. HEK293 cells were seeded onto poly(D-lysine)-coated cover glasses (BD Biosciences, San Jose, CA), and then transfection was performed. Cells were washed twice in Tris-buffered saline (TBS), fixed for 1 min at room temperature in a mixture of methanol/acetone (1:1), and rewashed in TBS. The cells were incubated for 1 h at room temperature in TBS containing monoclonal anti-FLAG M2-FITC antibody (Sigma) (1:1000). Cells were thoroughly washed, and coverslips were mounted. These samples were examined with Eclipse E800 fluorescence microscope (Nikon, Tokyo, Japan) equipped with MRC-1024 laser confocal system (Bio-Rad Laboratories).

Statistical Analysis. The significance of differences between the wild-type and mutant were analyzed using Dunnett's post hoc analysis. Two or three experiments were conducted, and representative

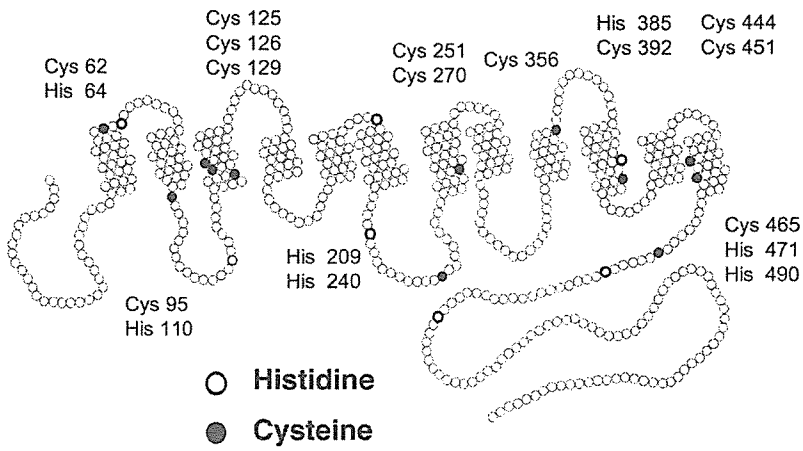

Fig. 1. Putative secondary structure of rMATE1 protein. The histidine (O) and cysteine (●) residues conserved among species are shown.

balt5/zmo-mol/zmo-mol/zmo00607/zmo5162-07a | ironmong | S=5 | 3/19/07 | 10:09 | 4/Color Figure(s): 6 | Art: 032938 | Input-kag

results are shown. Other analyses were conducted with Student's *t* test.

Results

Transport Analysis of rMATE1 Histidine and Cysteine Mutants. When amino acid sequences of rat, human, and mouse MATE1 were compared, 7 histidine and 12 cysteine residues were found to be conserved. Figure 1 shows the location of these amino acids in the predicted secondary structure of rMATE1. To determine which residues are essential for the transport activity of rMATE1, conserved histidine and cysteine residues were changed to glutamine and glycine residues, respectively. As shown in Fig. 2A, [^{14}C]TEA uptake was significantly reduced only in the rMATE1 H385Q among histidine mutants. As for cysteine mutants, the transport activity of C62G and C126G mutants was remarkably reduced, and [^{14}C]TEA uptake by C129G, C356G, C392G, and C451G mutants was significantly but modestly inhibited (Fig. 2B). We then focused on the amino acid residues His-385, Cys-62, and Cys-126 and further evaluated their functional importance. The substitution of these three amino acid residues in rMATE1 for other amino acid residue also abolished [^{14}C]TEA uptake (Fig. 3). These three amino acid residues are also conserved in hMATE1 (His-386, Cys-63, and Cys-127) and hMATE2-K (His-382, Cys-59, and Cys-123), and therefore, histidine and cysteine mutants of hMATE1 and hMATE2-K were prepared. As shown in Fig. 4, the transport of [^{14}C]TEA via the hMATE1 and hMATE2-K mutants was also diminished, suggesting that these histidine and cysteine amino acid residues are essential to the MATE families.

Protein Expression of rMATE1 Mutants. One possible reason for the defective transport activity of these mutants is a decreased level of the mutant protein in the plasma membranes of HEK293 cells, which could be caused by reduced stability and/or impaired insertion into the membranes of the mutants. To examine this possibility, Western blot analyses of plasma membranes prepared from each rMATE1 mutant and the immunolocalization of rMATE1 mutants were performed. Cell surface biotinylation was performed to specifically capture plasma membranes, and biotinylation techniques were confirmed to detect Na^+/K^+-ATPase for all samples (Goel et al., 2005). As shown in Fig. 5, all MATE1 mutant proteins were expressed at plasma membranes and wild-type MATE1. Furthermore, immunofluorescence analyses with confocal microscopy revealed that the rMATE1 mutant proteins with H385Q, C62G, and C126G were localized

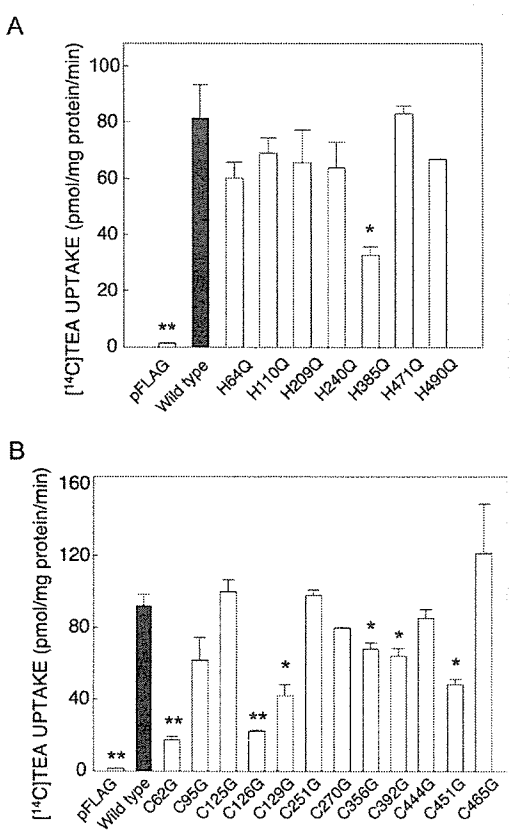

Fig. 2. Uptake of [^{14}C]TEA by HEK293 cells expressing wild-type and histidine (A) or cysteine (B) mutants of rMATE1. The cells were preincubated with incubation medium, pH 7.4, in the presence of 30 mM ammonium chloride for 20 min. Then the preincubation medium was removed, and the cells were incubated with 5 μM [^{14}C]TEA (10.36 kBq/ml, pH 7.4) for 1 min at 37°C. Each column represents the mean ± S.E. of three monolayers. This figure is a representative one from three separate experiments. *, $p < 0.05$, **, $p < 0.01$, significantly different from the wild type.

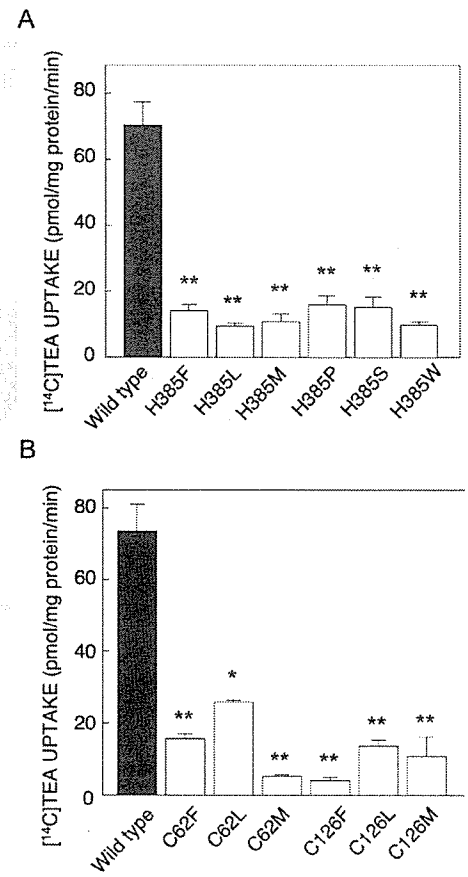

Fig. 3. Effect of various amino acid substitutions of His-385 (A), Cys-62, and Cys-126 (B) of rMATE1 on the uptake of [^{14}C]TEA by HEK293 cells expressing each rMATE1 mutant. The cells were preincubated with incubation medium, pH 7.4, in the presence of 30 mM ammonium chloride for 20 min. Then the preincubation medium was removed, and the cells were incubated with 5 μM [^{14}C]TEA, pH 7.4, for 1 min at 37°C. Each column represents the mean ± S.E. for three monolayers. This figure is a representative one from three separate experiments. *, $p < 0.05$, **, $p < 0.01$, significantly different from the wild type.

F6 at the plasma membranes (Fig. 6). Although intracellular staining in addition to membrane labeling was observed, this might be caused by the overexpression of rMATE1. This issue of expression pattern could not be ruled out in the transient expression system. These findings suggested that the low levels of transport activity of rMATE1 mutants with H385G, C62G, and C126G were not caused by the alteration of protein expression in plasma membranes.

Effects of DEPC or PCMBS Treatment on rMATE1 Function. We next examined the functional roles of the cysteine and histidine residues by using chemical modifiers such as the sulfhydryl reagent PCMBS and the histidine F7 residue modifier DEPC. As shown in Fig. 7, pretreatment of rMATE1-expressing cells with PCMBS or DEPC led to a concentration-dependent decrease in the transport of [^{14}C]TEA. The half-maximal inhibition for [^{14}C]TEA transport via rMATE1 was calculated as 1.13 ± 0.91 mM for DEPC and 37.2 ± 10.2 μM for PCMBS.

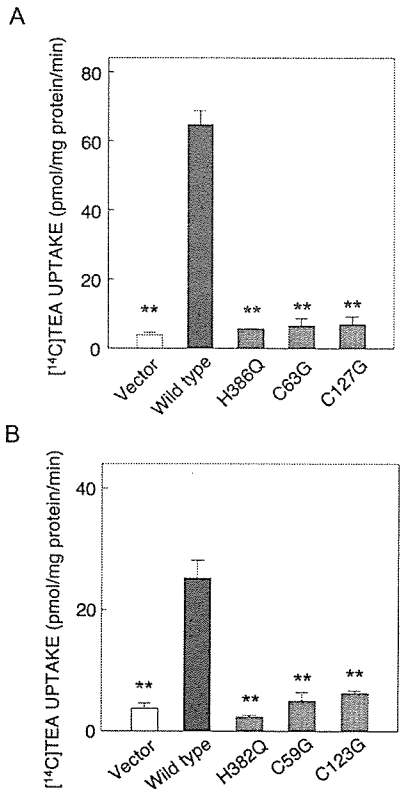

Fig. 4. Uptake of [^{14}C]TEA by HEK293 cells expressing wild-type and histidine and cysteine mutants of hMATE1 (A) or hMATE2-K (B). The cells were preincubated with incubation medium, pH 7.4, in the presence of 30 mM ammonium chloride for 20 min. Then the preincubation medium was removed, and the cells were incubated with 5 μM [^{14}C]TEA, pH 7.4, for 1 min at 37°C. Each column represents the mean ± S.E. of three monolayers. This figure is a representative one from two separate experiments. **, $p < 0.01$, significantly different from wild type.

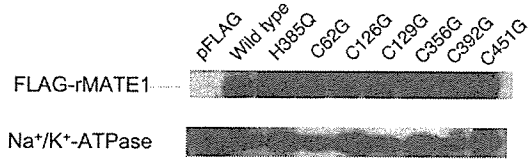

Fig. 5. Western blot analysis of plasma membranes obtained from HEK293 cells transiently expressing wild-type rMATE1 or histidine or cysteine mutants of rMATE1. Plasma membrane fractions prepared by cell surface biotinylation were separated by SDS-polyacrylamide gel electrophoresis (10%) and blotted onto polyvinylidene difluoride membranes. Monoclonal anti-FLAG-M2 antibody or Na^+/K^+-ATPase antibody was used as a primary antibody. A horseradish peroxidase-conjugated anti-mouse IgG antibody was used for detection of the bound antibody, and the strips of blots were visualized by chemiluminescence on X-ray film.

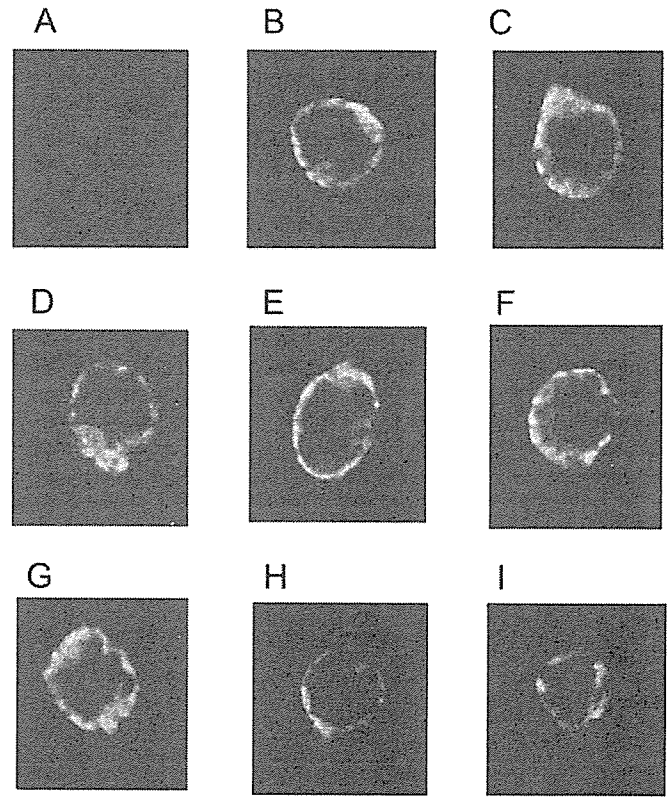

Fig. 6. Localization of FLAG-rMATE1 protein in HEK293 cells transiently transfected with vector alone (A), wild-type rMATE1 (B), or the H385Q (C), C62G (D), C126G (E), C129G (F), C356G (G), C392G (H), or C451G (I) mutant observed by confocal microscopy. HEK293 cells transfected with vector alone, wild-type cDNA, and mutant rMATE1 cDNA were fixed and stained with monoclonal anti-FLAG M2-FITC antibody.

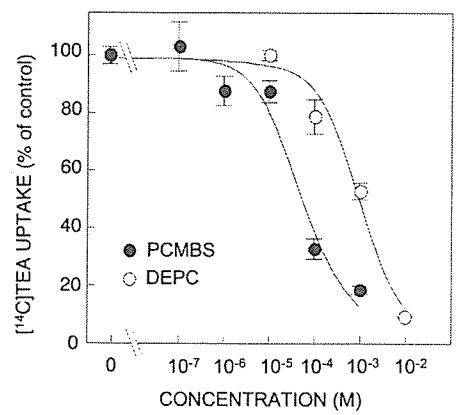

Fig. 7. Effects of DEPC (○) and PCMBS (●) on the uptake of TEA by rMATE1-expressing HEK293 cells. FLAG-rMATE1 cDNA was transfected into the HEK293 cells. The cells were preincubated at 25°C for 10 min with various concentrations of DEPC, pH 6.0, or PCMBS, pH 7.4. After incubation, the cells were rinsed twice with incubation medium and preincubated with incubation medium, pH 7.4, in the presence of 30 mM ammonium chloride for 20 min. Then the preincubation medium was removed, and the cells were incubated with 5 μM [^{14}C]TEA, pH 7.4, for 1 min at 37°C. Each point represents the mean ± S.E. of three monolayers. This figure is a representative one from three separate experiments.

balt5/zmo-mol/zmo-mol/zmo00607/zmo5162-07a | ironmong | S=5 | 3/19/07 | 10:09 | 4/Color Figure(s): 6 | Art: 032938 | Input-kag

Effect of DEPC or PCMBS in the Presence of Unlabeled TEA on rMATE1. We examined the effect of DEPC or PCMBS pretreatment in the presence of unlabeled TEA on rMATE1 function. As shown in Fig. 8A, unlabeled TEA had no effect on the inhibition of [^{14}C]TEA uptake by DEPC. On the other hand, unlabeled TEA protected against the inhibition of [^{14}C]TEA uptake caused by PCMBS pretreatment (Fig. 8B). The PCMBS-caused inhibition of [^{14}C]TEA transport via rMATE1 was also blocked by an excess of other MATE1 substrates such as cephalexin, cimetidine, and metformin but not by a typical organic anion, PAH. The results suggest that cysteine residues in rMATE1 interact with the substrates.

We further examined the protective effect of unlabeled TEA on [^{14}C]TEA uptake by C62G and C126G mutants treated with PCMBS (0.1 mM). [^{14}C]TEA uptake by C62G or C126G mutant was significantly decreased by the pretreatment of PCMBS (C62G: 7.52 ± 1.68 to 1.68 ± 0.13 pmol/mg of protein/min, $p < 0.05$; C126G: 8.68 ± 0.17 to 2.72 ± 0.09 pmol/mg of protein/min, $p < 0.05$, mean ± S.E., $n = 3$), indicating that cysteine residues other than Cys-62 and Cys-126 were sensitive to PCMBS. In contrast to wild-type rMATE1, the PCMBS-caused inhibition of [^{14}C]TEA uptake in these cysteine mutants was not protected by unlabeled TEA (C62G, 1.70 ± 0.19 pmol/mg of protein/min; C126G, 2.55 ± 0.41 pmol/mg of protein/min; mean ± S.E., $n = 3$). These results raised the possibility that at least both Cys-62 and Cys-126 contributed to the substrate binding.

pH Profile of TEA Uptake by rMATE1 H385Q. To investigate the role of the histidine residues, the pH profile of the uptake of [^{14}C]TEA by the rMATE1 H385Q mutant was examined. When the extracellular pH was changed from 6.0 to 8.5, the transport of [^{14}C]TEA by wild-type rMATE1 showed a bell-shaped curve with the greatest uptake value at pH 7.5. On the other hand, in the case of rMATE1 H385Q, no peak of the uptake was observed (Fig. 9).

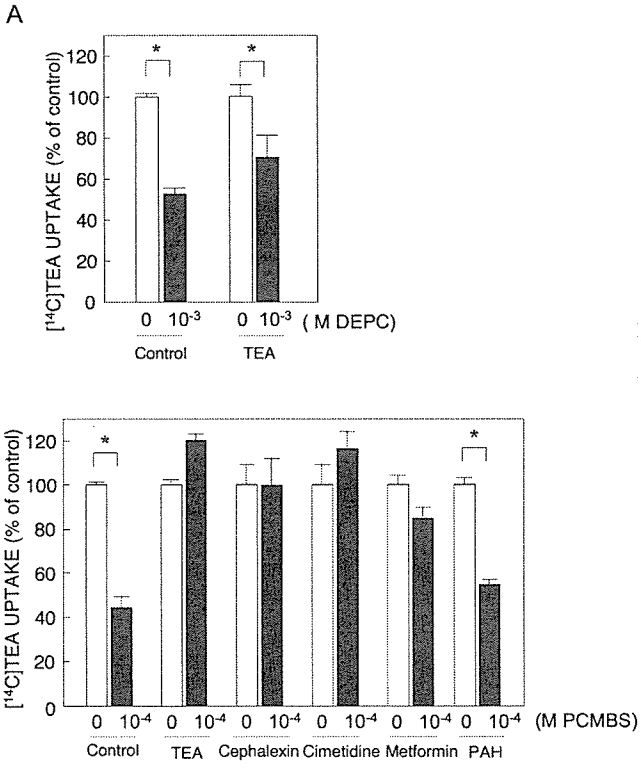

Fig. 8. Effects of unlabeled compounds on the inhibition of [^{14}C]TEA uptake by DEPC (A) or PCMBS (B)-pretreated rMATE1-expressing HEK293 cells. The cells were preincubated at 25°C for 10 min with or without unlabeled TEA (10 mM) and DEPC (1 mM), pH 6.0 (A) or were preincubated at 25°C for 10 min with or without unlabeled compounds (10 mM TEA, cephalexin, metformin, and PAH or 10 μM cimetidine) and PCMBS (0.1 mM) pH 7.4 (B). After the incubation, the cells were rinsed twice with incubation medium and preincubated with incubation medium, pH 7.4, in the presence of 30 mM ammonium chloride for 20 min. Then the preincubation medium was removed, and the cells were incubated with 5 μM [^{14}C]TEA, pH 7.4, for 1 min at 37°C. Each column represents the mean ± S.E. of three monolayers. This figure is a representative one from two separate experiments. *, $p < 0.05$, significantly different from wild type.

Discussion

Recent molecular biological approaches have revealed that the mammalian MATE family functions as the renal H^+/organic cation antiport system. MATE1 can transport not only a typical organic cation TEA (Otsuka et al., 2005a; Ohta et al., 2006; Terada et al., 2006) but also various cationic drugs such as cimetidine and metformin and zwitter ion cephalexin (Terada et al., 2006). Furthermore, we recently found that hMATE1 also transports platinum agents (Yonezawa et al., 2006). To understand the molecular mechanisms behind the multispecificity of MATE1, it is necessary to define substrate-binding and/or recognition sites located in the transporter protein. Among amino acid residues, cysteine and histidine are of interest because we found previously that sulfhydryl groups and histidine residues are essential for the transport activity of H^+/organic cation antiport system using rat renal brush-border membrane vesicles (Hori et al., 1987, 1989) and a pig kidney epithelial cell line, LLC-PK_1 (Inui et al., 1985; Saito et al., 1992). Based on these backgrounds, in the present study, functional roles of cysteine and histidine residues of the MATE family, especially rMATE1, were examined.

By mutational analysis, we found that Cys-62 and Cys-126 of rMATE1, which are located in the first and the third

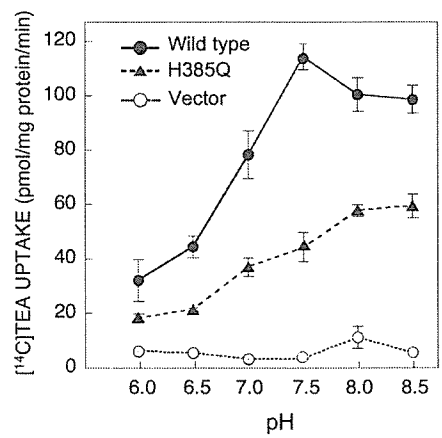

Fig. 9. Uptake of [^{14}C]TEA by HEK293 cells expressing wild-type rMATE1 (●), the H385Q mutant (▲), or vector alone (○). The cells were preincubated with incubation medium, pH 7.4, in the presence of 30 mM ammonium chloride for 20 min. Then the preincubation medium was removed, and the cells were incubated with 5 μM [^{14}C]TEA, (pH 6.0 to 8.5, for 1 min at 37°C. Each point represents the mean ± S.E. of three monolayers. This figure is a representative one from two separate experiments.

transmembrane domain, respectively, played critical roles in the transport activity of TEA (Figs. 1 and 2). It is interesting that the corresponding cysteine residues of hMATE1 and hMATE2-K also function as essential amino acid residues (Fig. 4), suggesting that these cysteine residues play critical roles in the MATE family. Furthermore, protection by the substrate against PCMBS-caused inhibition of the transport of TEA via rMATE1 (Fig. 8) suggested that cysteine residues of rMATE1 function as substrate-binding sites. Protection assay using rMATE1 C62G and C126G mutants suggested that both Cys-62 and Cys-126 are involved in the substrate binding, although we cannot rule out the possibility that other cysteine residues participated in the substrate recognition. Pelis et al. (2006) have recently found that Cys-474 of hOCT2, which is suggested to be located in the 11th transmembrane helix that participates in the formation of the hydrophilic cleft, contributes to substrate-protein interaction. Because OCTs and MATEs have similar substrate specificity, although their driving forces are quite different, it is reasonable that the same amino acid cysteine is involved in the substrate recognition. The present results strongly suggest that Cys-62 and Cys-126 of rMATE1 play an important role for substrate-interaction sites.

Most of the His-385 mutants of rMATE1 (Figs. 2 and 3) and corresponding histidine mutants of hMATE1 and hMATE2-K (Fig. 4) did not have the TEA transport activity. Furthermore, the histidine modifier reagent DEPC also inhibited the transport of TEA via rMATE1 (Fig. 7). In contrast to the effect of PCMBS, the DEPC-caused inhibition of TEA transport was not blocked in the presence of excess TEA (Fig. 8), suggesting that histidine residue of rMATE1 does not serve as substrate-binding site. In other H^+-coupled transporters such as H^+/peptide cotransporter 1 (Uchiyama et al., 2003) and Na^+/H^+ exchanger (Cha et al., 2003), histidine residues function as an H^+-binding site. It is, therefore, suggested that histidine residue of the MATE family acts as a H^+-binding site for driving force.

The H^+/organic cation antiport system is very sensitive to pH. The uptake of TEA was optimal at pH 7.0, and the uptake was markedly decreased at either an acidic or alkaline pH in renal brush-border membrane vesicle (Maegawa et al., 1988). No peak in the uptake of TEA by the rMATE1 H385Q mutant was observed when the pH of the medium changed gradually (Fig. 9). His-385 of rMATE1 may be important to the bell-shaped transport activity and function not only in making the driving force but as a regulator of substrate transport. Further studies such as detailed kinetic analyses may be needed. To our knowledge, there has been no report that a histidine residue is involved in the transport of a substrate by the MATE family.

Site-directed mutagenesis revealed that Asp-32, Glu-251, and Asp-367 of NorM protein, which is a member of the *Vibrio parahaemolyticus* MATE family, are essential for the Na^+-driven organic cation export (Otsuka et al., 2005b). Mutated hMATE1 with Glu-273 replaced with glutamine, the counterpart of Glu-251 of NorM protein, lacked TEA transport activity (Otsuka et al., 2005a). This glutamate residue is also conserved among rMATE1, mMATE1, and hMATE2-K. Previous studies using renal brush-border membrane vesicles treated with chemical modifiers revealed that carboxylate groups are critical for transport activity but are not involved in the substrate binding (Sokol et al., 1987). Alternatively, it was speculated that carboxylate groups are responsible for H^+ translocation process. It is therefore suggested that cysteine residues in the mammalian MATE family play a more important role for the substrate recognition than other amino acid residues. In MATE1, cysteine residues are located in the first and third transmembrane domains. The development of a three-dimensional model of MATE1 will clarify the molecular interaction of these amino acid residues with cationic substrates, as proposed for rat OCT1 (Popp et al., 2005) and rabbit OCT2 (Zhang et al., 2005). AQ: A

In conclusion, we demonstrated that His-385, Cys-62, and Cys-126 in rMATE1 and corresponding amino acid residues of hMATE1 and hMATE2-K play an important role for the transport activity of MATE family. Cysteine residues of MATE1 make a key contribution to substrate recognition. This is the first study to identify the histidine and cysteine residues essential to the mammalian MATE family.

References

Burckhardt G and Wolff NA (2000) Structure of renal organic anion and cation transporters. *Am J Physiol* **278:**F853–F866.

Cha B, Oh S, Shanmugaratnam J, Donowitz M, and Yun CC (2003) Two histidine residues in the juxta-membrane cytoplasmic domain of Na^+/H^+ exchanger isoform 3 (NHE3) determine the set point. *J Membr Biol* **191:**49–58.

Goel M, Shinkins W, Keightley A, Kinter M, and Schilling WP (2005) Proteomic analysis of TRPC5- and TRPC6-binding partners reveals interaction with the plasmalemmal Na^+/K^+-ATPase. *Pflueg Arch Eur J Physiol* **451:**87–98.

Hiasa M, Matsumoto T, Komatsu T, and Moriyama Y (2006) Wide variety of locations for rodent MATE1, a transporter protein that mediates the final excretion step for toxic organic cations. *Am J Physiol* **291:**C678–C686.

Hong M, Zhou M, and You G (2004) Critical amino acid residues in transmembrane domain 1 of the human organic anion transporter hOAT1. *J Biol Chem* **279:** 31478–31482.

Hori R, Maegawa H, Kato M, Katsura T, and Inui K (1989) Inhibitory effect of diethyl pyrocarbonate on the H^+/organic cation antiport system in rat renal brush-border membranes. *J Biol Chem* **264:**12232–12237.

Hori R, Maegawa H, Okano T, Takano M, and Inui K (1987) Effect of sulfhydryl reagents on tetraethylammonium transport in rat renal brush border membranes. *J Pharmacol Exp Ther* **241:**1010–1016.

Inui K, Masuda S, and Saito H (2000) Cellular and molecular aspects of drug transport in the kidney. *Kidney Int* **58:**944–958.

Inui K and Okuda M (1998) Cellular and molecular mechanisms of renal tubular secretion of organic anions and cations. *Clin Exp Nephrol* **2:**100–108.

Inui K, Saito H, and Hori R (1985) H^+-gradient-dependent active transport of tetraethylammonium cation in apical-membrane vesicles isolated from kidney epithelial cell line LLC-PK_1. *Biochem J* **227:**199–203.

Maegawa H, Kato M, Inui K, and Hori R (1988) pH sensitivity of H^+/organic cation antiport system in rat renal brush-border membranes. *J Biol Chem* **263:**11150–11154.

Masuda S, Terada T, Yonezawa A, Tanihara Y, Kishimoto K, Katsura T, Ogawa O, and Inui K (2006) Identification and functional characterization of a new human kidney-specific H^+/organic cation antiporter, kidney-specific multidrug and toxin extrusion 2. *J Am Soc Nephrol* **17:**2127–2135.

Ohta K, Inoue K, Hayashi Y, and Yuasa H (2006) Molecular identification and functional characterization of rat MATE1 as an organic cation/H^+ antiporter in the kidney. *Drug Metab Dispos* **34:**1868–1874.

Otsuka M, Matsumoto T, Morimoto R, Arioka S, Omote H, and Moriyama Y (2005a) A human transporter protein that mediates the final excretion step for toxic organic cations. *Proc Natl Acad Sci USA* **102:**17923–17928.

Otsuka M, Yasuda M, Morita Y, Otsuka C, Tsuchiya T, Omote H, and Moriyama Y (2005b) Identification of essential amino acid residues of the NorM Na^+/multidrug antiporter in *Vibrio parahaemolyticus*. *J Bacteriol* **187:**1552–1558.

Pelis RM, Zhang X, Dangprapai Y, and Wright SH (2006) Cysteine accessibility in the hydrophilic cleft of the human organic cation transporter 2. *J Biol Chem* **281:**35272–35280.

Popp C, Gorboulev V, Muller TD, Gorbunov D, Shatskaya N, and Koepsell H (2005) Amino acids critical for substrate affinity of rat organic cation transporter 1 line the substrate binding region in a model derived from the tertiary structure of lactose permease. *Mol Pharmacol* **67:**1600–1611.

Saito H, Yamamoto M, Inui K, and Hori R (1992) Transcellular transport of organic cation across monolayers of kidney epithelial cell line LLC-PK_1. *Am J Physiol* **262:**C59–C66.

Sokol PP, Holohan PD, and Ross CR (1987) N,N′-Dicyclohexylcarbodiimide inactivates organic cation transport in renal brush border membranes. *J Pharmacol Exp Ther* **243:**455–459.

Terada T, Masuda S, Asaka J, Tsuda M, Katsura T, and Inui K (2006) Molecular cloning, functional characterization and tissue distribution of rat H^+/organic cation antiporter MATE1. *Pharm Res (NY)* **23:**1696–1701.

Terada T, Saito H, Mukai M, and Inui K (1996) Identification of the histidine